

Scales of Variability of Bio-Optical Properties as Observed from Near-Surface Drifters

MARK R. ABBOTT,¹ KENNETH H. BRINK,² C. R. BOOTH,³ DOLORS BLASCO,⁴
MARK S. SWENSON,⁵ CURTISS O. DAVIS,⁶ AND L. A. CODISPOTI⁷

A drifter equipped with bio-optical sensors and an automated water sampler was deployed twice, in 1987 and 1988, in the California Current as part of the Coastal Transition Zone program to study the biological, chemical, and physical dynamics of the meandering filaments observed off northern California. Measurements were made of fluorescence, downwelling irradiance, upwelling radiance, and beam attenuation using several bio-optical sensors. Samples were collected by an automated sampler for later analysis of nutrients and phytoplankton species composition. Large scale spatial and temporal changes in the bio-optical and biological properties of the region were driven by changes in ocean circulation associated with the meanders. Variance spectra of the bio-optical parameters revealed fluctuations on both diel and semi-diurnal scales associated with solar variations and internal tides, respectively. Offshore, inertial motions were apparent in the variance spectra of temperature, fluorescence and beam attenuation. Although calibration samples can help remove some of these variations, these results suggest that the use of bio-optical data from unattended platforms such as moorings and drifters must be analyzed carefully. Characterization of the scales of phytoplankton variability must also account for the scales of variability in the algorithms used to convert bio-optical measurements into biological quantities.

1. INTRODUCTION

Satellite observations of ocean color provide a unique view of the large-scale patterns of phytoplankton pigment in the upper ocean. Coupled with increasingly sophisticated numerical models, there is now the potential to study basin-scale and global scale biogeochemical processes in the ocean in greater detail than before. However, obstacles remain, especially in the parameterization of the unresolved scales. Similar problems confront models of ocean physics. For example, the parameterization of small-scale turbulence and diffusion significantly affects the large-scale patterns of heat flux [Bryan, 1987]. The characterization of small-scale variability is also necessary for optimal interpolation of sparse data sets. Chelton and Schlax [1991] used estimates of the variance spectrum to derive optimal estimates of mean fields for irregularly sampled time series. They used a sequence of coastal zone color scanner (CZCS) imagery to show that simple means provide little information in cases where there are long gaps in the series. Using maps of field measurements, Denman and Freeland [1985] estimated the structure functions of chlorophyll and a set of physical variables to produce objective maps. Thus both parameterization for models and optimal estimates for temporal and spatial fields rely on estimates of the sub-grid scale variability in order to map the larger scale fields of interest.

Such small-scale variability is more than merely a nuisance for sampling and modeling. As phytoplankton growth rates respond on scales of a day or less (and hence on spatial scales of tens of kilometers), this sub-grid scale is likely the focus of physical/biological coupling [Denman and Powell, 1984; Harris, 1986; Abbott, 1993]. As these scales are difficult to observe, it is essential that we begin to characterize this variability sufficiently to derive statistically robust fields and models at larger scales.

Bio-optical measurements have been used for decades as surrogates for direct measurements of biological properties [Zaneveld, 1989; Smith et al., 1991]. With improvements in data storage, batteries, and sensor design, routine bio-optical measurements can be made from unattended platforms such as

moorings and drifters [Dickey, 1991]. Such observation strategies now allow the study of processes that were previously difficult to resolve using conventional shipboard techniques [Dickey et al., 1991; Smith et al., 1991]. With their ability to resolve small-scale variability, these strategies will allow us to derive statistics necessary for techniques such as optimal interpolation.

During the spring/summer upwelling season, large meanders are apparent in the California Current [Strub et al., 1991]. Inshore of these meanders, cold water is present near the surface and is characterized by high nutrient and chlorophyll concentrations. The Coastal Transition Zone program was designed to characterize the physical, biological, and chemical dynamics of these meanders or filaments [Brink and Cowles, 1991]. Using an array of bio-optical sensors and automated water sampler, a drifter (drogue depth 13 m) was deployed once in 1987 and once in 1988. The water-following characteristics of these drifters potentially allow separation of temporal variability from spatial variability [Niiler et al., 1987; Paduan and Niiler, 1990; Brink et al., 1991; Swenson et al., 1992] although vertical water movements will appear as temporal variations because the instruments are drogued at a constant depth. This meandering region is the site of relatively large vertical excursions, on the order of several tens of meters per day [Washburn et al., 1991; Kadko et al., 1991; Swenson et al., 1992]. Thus estimates of the time scales of variability will include the scales of vertical motion as well as the scales associated with bio-optical changes in a particular water mass.

We compared several methods to derive biological properties, such as chlorophyll concentration and primary productivity, from the basic bio-optical signals. Although we were not able to derive estimates of absolute error, we were able to estimate the relative variability between the different methods on scales of days. There were also considerable differences between the two deployments in the bio-optical properties of the phytoplankton which were apparent in these functional relationships. We suspect that these are largely driven by shifts in species composition and hence affect the bio-optical properties.

We use standard time series techniques to study the characteristics scales of variability. These results were compared

with measurements of the physical environment to estimate the degree of coupling between physical and bio-optical variability. There is strong interaction between physical forcing and bio-optical properties at a wide range of time scales. Future sampling programs, especially those relying on satellite remote sensing, must take such small-scale variability into account when scaling up to large-scale models.

2. METHODS

The drifter used in this study has been described by *Niiler et al.* [1987], *Paduan and Niiler* [1990], and *Swenson et al.* [1992]. The instrumentation consisted of a spectroradiometer, beam transmissometer, and a strobe fluorometer. Details of the bio-optical instrumentation can be found in *Abbott et al.* [1990]. An automated water sampler [*Friederich et al.*, 1986] was used to collect samples for later nutrient and phytoplankton analyses. The configuration of the drifter and the specific sampling techniques are described by *Abbott et al.* [1990]. The bio-optical sampler was at 8.5 m and the water sampler was at 17.5 m. Bio-optical samples were collected every 4 minutes after averaging for 45 seconds, and water samples were collected every 12 hours. In 1988, samples were collected adjacent to the drifter at noon every day for shipboard analysis. Water samples were collected from the ship only at the beginning and end of the 1987 deployment. These samples were used to estimate chlorophyll concentrations using standard extraction methods.

We used several algorithms to convert the bio-optical measurements into estimates of chlorophyll. The most obvious was to convert the strobe fluorometer data using the chlorophyll extractions as calibration points. Clearly, this method would not be accurate in 1987 when samples were collected only at the beginning and end of the deployment.

The sun-stimulated fluorescence method was based on the model described in *Kiefer et al.* [1989] and *Chamberlin et al.* [1990]. The flux of sun-stimulated fluorescence (F_f) was calculated as follows:

$$F_f = 4\pi(k(PAR) + a(Chl)) * L_u(Chl) \quad (1)$$

where $k(PAR)$ is the diffuse attenuation for scalar irradiance between 400 and 700 nm [*Kiefer et al.*, 1989], $a(Chl)$ is the total absorption coefficient, and $L_u(Chl)$ is the spectrally-integrated radiance of a chlorophyll-like substance. The 4π term is a geometric constant that transforms the radiance to a volume emission (with units of steradians, not str^{-1} as described by *Chamberlin et al.* [1990]). F_f was converted to chlorophyll as

$$Chl = \frac{F_f}{E_o(PAR) * \phi_f * \sigma_{ac}(PAR)} \quad (2)$$

where $E_o(PAR)$ is the downwelling scalar irradiance between 400 and 700 nm, ϕ_f is the quantum yield of fluorescence, and σ_{ac} is specific absorption coefficient of phytoplankton.

In (1), we followed *Kiefer et al.* [1989] and assumed that $k(PAR) + a(Chl) \approx 0.52$. This assumption works fairly well in waters where $Chl < 2.0 \text{ mg/m}^3$, a condition that was not always met in the study area. Assuming other

parameters remain constant, this will result in an underestimate of chlorophyll concentrations in regions with $> 2.0 \text{ mg/m}^3$.

$E_o(PAR)$ was based on a linear regression of the downwelling irradiance at 520 nm, $E_d(520)$, using

$$E_o(PAR) = -0.0011 + .00245 * E_d(520) \quad (3)$$

We compared this method with an estimate of the integrated radiance between 400 and 700 nm using the full spectroradiometric data. The correlation between the two estimates was 0.9996.

Following the methods described by *Siegel et al.* [1989], we used measurements of the beam attenuation to estimate chlorophyll. After converting the raw transmissometer data to beam attenuation using the methods of *Bartz et al.* [1978], we used the equations of *Bishop* [1986] where

$$SPM = (c - c_w) * k \quad (4)$$

In (4) SPM is suspended particulate matter, c is the beam attenuation coefficient, c_w is the beam attenuation resulting from pure water, and k is an empirical coefficient relating beam attenuation to SPM . Based on *Bishop's* data, we used $k = 1150$. Following *Bishop* [1986], we assumed that approximately 25% of the SPM was carbon. We then converted this carbon estimate to chlorophyll, using a carbon:chlorophyll ratio of 60. As the beam transmissometer failed in the 1988 deployment, we present results only from 1987.

The last method used to estimate chlorophyll concentration was based on irradiance ratios as described by *Smith et al.* [1991]. Although upwelling radiance is far more sensitive to changes in chlorophyll concentration, downwelling irradiance was used with some success on the BIOWATT moorings by *Smith et al.* [1991]. We estimated Chl as

$$Chl = A \left[\frac{E_d(441)}{E_d(520)} \right]^B \quad (5)$$

E_d is the downwelling irradiance at 441 and 520 nm and A and B are fitted parameters. *Smith et al.* [1991] report values for A and B at 32, 52, and 72 m depth from the BIOWATT mooring.

We estimated the total backscattering coefficient using two methods. The first method relied on the beam attenuation measurements, and the second method was based on chlorophyll and wavelength-dependent coefficients. The beam attenuation coefficient can be expressed as

$$c = a + b \quad (6)$$

where a is absorption coefficient and b is the scattering coefficient. Scattering is defined as the sum of the forward scattering component, b_f , and the backscattering component, b_b . As described by *Kirk* [1983], the absorption coefficient can be approximated as

$$R \approx 0.33 \frac{b_b}{a} \quad (7)$$

where R is the ratio of the upwelling to downwelling irradiance (often denoted as remote sensing reflectance). We can rearrange (6) and (7) such that

$$c = \left(\frac{.33}{R} + 1 + \frac{b_f}{b_b} \right) b_b \quad (8)$$

Assuming that $\frac{b_f}{b_b} \approx 100$, then backscattering at particular wavelength can be approximated as

$$b_b \approx \left(\frac{c}{\frac{.33}{R} + 100} \right) \quad (9)$$

Although we did not make direct measurements of upwelling irradiance, E_u can be approximated from the upwelling radiance measurements as

$$E_u \approx 5 \times L_u \quad (10)$$

where L_u is upwelling radiance [Kirk, 1983].

These estimates of backscatter were compared with those based on chlorophyll, as described by Gordon *et al.* [1988]. The backscattering coefficient was broken into the component due to phytoplankton ($(b_b)_p$) and that due to water ($(b_b)_w$) as follows

$$b_b = (b_b)_p + (b_b)_w \quad (11)$$

Gordon *et al.* [1988] model the backscattering due to phytoplankton as

$$(b_b)_p = A(\lambda)C^{B(\lambda)} \quad (12)$$

where C is the chlorophyll concentration (in our case estimated from the strobe fluorometer measurements) and $A(\lambda)$ and $B(\lambda)$ are fitted for various wavelengths. As we had the requisite upwelling and downwelling measurements at only 441 and 550 nm, we estimated backscattering at only those two wavelengths.

We estimated instantaneous primary productivity based on the model described by Chamberlin *et al.* [1990] using sun-stimulated fluorescence. The rate of primary production can be expressed as

$$F_c = \left(\frac{k_{cf}}{k_{cf} + E_o(PAR)} \right) \times \left(\frac{\phi_c}{\phi_f} \right)_{max} \times F_f \quad (13)$$

where k_{cf} is the value of the irradiance at $1/2 (\phi_c/\phi_f)_{max}$, and $(\phi_c/\phi_f)_{max}$ is the maximum value of the ratio of the quantum yields of photosynthesis and fluorescence. Using the data described by Chamberlin *et al.* [1990], we assumed that $(\phi_c/\phi_f)_{max}$ was approximately $2.3 \text{ atoms C photon}^{-1} \text{ Ein m}^{-3} \text{ s}^{-1}$ and that k_{cf} was approximately $133 \text{ mEin m}^{-2} \text{ s}^{-1}$. After making the necessary unit conversions, we expressed the rate of primary production as $\text{ng-atm C m}^{-3} \text{ s}^{-1}$, consistent with Chamberlin *et al.* [1990].

For the 1987 deployment, it was possible to estimate the rate of primary production based on the change in water transparency using the beam attenuation measurements. We followed the method described by Siegel *et al.* [1989] whereby we converted the beam attenuation measurements to equivalent carbon estimates and then measured the change in carbon concentration over a four-hour period (from 1100 h to 1500 h, local time). We integrated the instantaneous productivities estimated from the sun-stimulated fluorescence method over the same four-hour period and then averaged them. This process gave us two estimates of hourly productivities between 1100 h and 1500 h in $\text{mg-at C m}^{-3} \text{ hr}^{-1}$.

We calculated variance spectra to estimate the time scales of variability, using maximum entropy techniques. Although this method may sometimes give misleading results, we focused our analysis on time scales greater than five hours so that the results are more robust. We also calculated structure functions which revealed the major scales of variability, but we do not present these results as they merely confirmed the patterns seen in the variance spectra.

3. RESULTS AND DISCUSSION

In both years, the drifter was deployed near an upwelling center at the nearshore end of a filament. The drifters were tracked via the Argos system. The two drifters followed the main axis of the filament offshore. Figure 1 shows the drifter tracks from 1987 and 1988. In both years, the drifters started nearshore, off Point Arena, and proceeded in a southward direction offshore. Both drifters stayed near the cold core of the meandering filament. The instrumented drifters tracked the water motion as well as the uninstrumented drifters [Swenson *et al.*, 1992]. During both deployments, the winds were generally southward in the range of 7–15 m/s.

3.1 Bio-optical Time Series

Figure 2 shows time series of temperature, strobe fluorescence, and $E_o(PAR)$ from the 1988 deployment. Plots of these variables from 1987 can be found in Abbott *et al.* [1990]. In both years the patterns of fluorescence and temperature were in general inversely related, as expected for upwelling regions [e.g., Hood *et al.*, 1990]. Temperature increased about 2°C in 1987 and about 3°C in 1988. As noted by Abbott *et al.* [1990], much of this increase was the result of convergence of warmer water along the path of the drifter in 1987, associated with a net downwelling of the surface water. Similar processes occurred in 1988, as Swenson *et al.* [1992] estimated that surface heating was in the range of 0.15 to 0.3°C/day , considerably less than the temperature change observed by the drifter.

Figure 3 shows chlorophyll estimated in 1987 using the strobe fluorescence, sun-stimulated fluorescence, beam attenuation, and irradiance ratio methods described earlier. We limited the estimates to the period from two hours before local solar noon to two hours after local solar noon (approximately 1100 h to 1500 h, local time). Note that the plots, however, show the time series as continuous functions with no gaps between successive midday periods. This minimized the effects of changing sun angle on the observed levels of irradiance. The irradiance ratios used the 72 m coefficients estimated by Smith *et al.* [1991]; the coefficients for 35 and 50 m resulted in significantly higher chlorophyll estimates. The sun-stimulated fluorescence data were converted to chlorophyll using a specific absorption coefficient (a_c) of 0.04 and a fluorescence efficiency (ϕ_f) of 0.045 as described by Kishino *et al.* [1984] and Collins *et al.* [1988]. We applied the coefficients described by Chamberlin *et al.* [1990] (0.016 and 0.028 for specific absorption and fluorescence efficiency) and found that the sun-stimulated fluorescence chlorophyll estimates were consistently higher than the strobe fluorescence estimates by a factor of three. We therefore

relied on the Kishino/Collins parameters for the sun-stimulated fluorescence model for the 1987 deployment.

Although there are differences in the four chlorophyll estimates, the general patterns of the four time series are similar. This similarity is particularly apparent in the early days of the deployment (days 168-171). The irradiance method is much less sensitive to changes in chlorophyll, especially in the low chlorophyll waters offshore. This is an expected result as the method is integrating downwelling irradiance over a very short distance. This is in contrast to the upwelling radiance method used in ocean color remote sensing in which the signal originates over 1-2 optical depths. The beam attenuation method also predicts much higher pigment values, but shows much of the same small-scale structure as the fluorescence methods. Note that the obvious discontinuities that appear in the latter stages of the deployment (days 172-175) are the result of limiting the data to near-noon observations. In particular, the discontinuity between day 172 and day 173 is especially abrupt. However, similar discontinuities are not apparent in the fluorescence methods. This point will be discussed below along with the monotonic increase in chlorophyll that is noticeable in days 173-175.

The two fluorescence methods are surprisingly similar over the duration of the deployment ($r^2=0.96$). Given that the strobe fluorescence data were "calibrated" (albeit limited) with chlorophyll extractions, we expect that these estimates are a reasonable measure of the 10 m chlorophyll record along the drifter track. The patterns are quite similar to the chlorophyll map derived by Hood *et al.* [1990] for this region. Relying on the fluorescence-based estimates, chlorophyll concentrations are initially moderate at the beginning of the deployment, increase rapidly, and then decrease precipitously. The high chlorophyll values nearshore from the transmissometer data are likely an artifact of the high particulate, but non-fluorescent, concentrations in the upwelling center [Abbott *et al.*, 1990].

Despite the numerous assumptions in the transmissometer-based chlorophyll estimates (coefficients for converting beam transmission to suspended particulate matter, to carbon, and finally to chlorophyll), the fluorescence methods and the transmissometer method are remarkably similar, differing by a factor of two to three. Although this is a large difference for in situ sampling, the discrepancy is in line with other remote sensing methods such as satellites [Gordon *et al.*, 1983].

The temporal patterns of the backscatter coefficients (Figure 4) are similar using the attenuation and chlorophyll-based models. The estimates are within the range measured in similar oceanographic conditions [e.g., Morel and Bricaud, 1981]. As expected, the general patterns follow the changes in chlorophyll. Note that in the middle of day 172 there is a sharp drop in the beam attenuation backscatter estimate. As this drop also appears in the beam attenuation chlorophyll estimate (Figure 3), this suggests that there is a strong change in the scattering properties which is not reflected in changes in chlorophyll (based on the other estimates). Abbott *et al.* [1990] showed that the phytoplankton community became dominated by large centric diatoms on this day, with a corresponding increase in cell volume (see Figures 10 and 12 in Abbott *et al.* [1990]). Backscatter should decrease with cell size [Bricaud *et al.*, 1988], which is consistent with our observations.

On the last three days of the deployment, backscatter (based

on beam attenuation) monotonically increases during the day. The patterns of chlorophyll derived from the two fluorescence methods (Figure 3) show a similar monotonic increase on day 175 but the previous two days are not as obvious. Abbott *et al.* [1990] interpreted these observations in terms of phytoplankton growth and subsequent grazing by zooplankton at night, similar to results from the oligotrophic central Pacific described by Siegel *et al.* [1989]. However, Cullen *et al.* [1992] note that near-surface scattering properties of phytoplankton can change dramatically during the day, thus confounding interpretations of scattering data. We suspect that similar changes may be occurring here, given the high light conditions on these days [Abbott *et al.*, 1990]. Upon closer examination of the beam attenuation model for backscatter, we found that the changes in b_b were dominated by changes in c (beam attenuation), not by changes in R , (reflectance).

The general patterns of chlorophyll were similar in 1988 (Figure 5), although the levels were much higher than in 1987 (Figure 3). The most noticeable difference is between the strobe fluorescence and the initial sun-stimulated fluorescence estimates. If we rely on the model coefficients presented by Kishino *et al.* [1984] and Collins *et al.* [1988], the sun-stimulated fluorescence estimates of chlorophyll are significantly lower than the calibrated (by daily in situ sampling next to the drifter) strobe fluorescence estimates by nearly a factor of three. This difference is then especially apparent nearshore in the high chlorophyll waters. We used different values for the specific absorption coefficient (a_c) and fluorescence efficiency (ϕ_f) of 0.016 and 0.028 based on work by Chamberlin *et al.* [1990] for which the match between these two fluorescence estimates is much better, especially during the first three days of the deployment. After day 188, the sun-stimulated fluorescence estimates using the Chamberlin coefficients are consistently higher than the strobe fluorescence estimates. Similar variability in these parameters and their effects on estimates of primary productivity from sun-stimulated fluorescence was observed by Stegmann *et al.* [1992].

These results suggest that there were significant changes in the fluorescence characteristics of the phytoplankton between the 1987 and 1988 deployments. The relationship between the two fluorescence estimates is much more complicated in 1988. First, recall that the strobe fluorescence estimates were "calibrated" against daily in situ observations; daily changes in this relationship can induce added variability. The strobe fluorescence calibration coefficient was much smaller on day 189 than at other times, perhaps accounting for at least part of the discrepancy between the two fluorescence methods. Second, changes in the sun-stimulated fluorescence model parameters are another source of variability. In addition to the apparently large shifts between 1987 and 1988, there appear to be changes in these parameters during the 1988 deployment. It is well known, for example, that fluorescence yield and specific absorption vary as a function of species composition [e.g., Bricaud *et al.*, 1988; Falkowski and Kiefer, 1985].

3.2 Phytoplankton Time Series

Figure 6 shows the 1988 phytoplankton species composition as a percentage of total cell volume. During the first three days

of the deployment, the phytoplankton community was dominated by *Chaetoceros* spp. and other centric diatoms. On day 189, the composition changed dramatically, with *Rhizosolenia* replacing *Chaetoceros*. The final shift was to a community dominated by dinoflagellates. Although a similar replacement of *Chaetoceros* by *Rhizosolenia* occurred in 1987 [Abbott *et al.*, 1990], the magnitude of the shift was not as dramatic. In 1987, the shift was from 35% *Chaetoceros* to 30% *Rhizosolenia* whereas the shift in 1988 was from 55% *Chaetoceros* to 45% *Rhizosolenia*. In 1987, the community was dominated by large centric diatoms in the offshore waters compared with dinoflagellates in 1988. Given the increased variability in species composition in 1988, it is not surprising to see large differences in the fluorescence response.

Changes in the physical environment are likely the ultimate cause of the species changes. Figure 2 shows the temperature changes along the drifter path. Before day 190, temperatures are cool and variable. The temperature increases sharply by 2° in 12 hours at day 190, and this front is associated with the shift to dinoflagellates (Figure 6). However, nutrients decrease rapidly before the temperature front is reached. Swenson *et al.* [1992] used two methods to estimate vertical velocities based on estimates of the heat budget and the vorticity budget. Although there were significant differences in the magnitude of the velocity estimates, the general patterns of upwelling and downwelling were quite similar. The larger estimates from the heat budget approach ranged from 70 m/day downwelling to 40 m/day upwelling whereas the vorticity estimates were about a factor of three smaller. However, as noted by Swenson *et al.* [1992], the heat budget estimates were based on a subcluster of drifters and represented a region of about 60 km² compared with 150 km² for the vorticity budget estimates. Initially, the bio-optical drifter was in a region of downwelling (about 40 m/day, based on the heat budget estimates) nearshore. This changed to moderate upwelling (about 20 m/day) on day 188. The drifter then experienced moderate downwelling about midway through day 188. Strong downwelling occurred during day 189 at the same time that *Chaetoceros* was replaced by *Rhizosolenia*. This downwelling was associated with an "instability" identified by Swenson *et al.* [1992] and a westward turn of the drifter. This was followed by weak upwelling on days 190 and 191 as dinoflagellates came to dominate the phytoplankton.

Given the complex flow patterns in this region, it is not surprising to see strong interleaving of various water masses characterized by different phytoplankton communities. Following the description laid out by Strub *et al.* [1991], we define the broad, cold, productive regions as the filaments which are separated from the warmer, less productive offshore waters by a meandering jet. As the drifter does not exactly follow a single water parcel, it may traverse these various water types. It is apparent from these data that the physical dynamics of the coastal transition zone affect the timing and nature of the species changes as observed by the drifter. Vertical sections of chlorophyll, temperature, and salinity, derived from the vertical profiles made at noon each day of the 1988 deployment next to the drifter, are shown in Figure 8. These show the strong front in temperature that occurred approximately 70 km along the drifter track on day 189 (Figure 2a). As *Rhizosolenia* are generally buoyant, their increase on day 189 in association with

this front is not unexpected.

The patterns of phytoplankton species (Figure 6, and Figure 12 of Abbott *et al.* [1990]) show some differences, although it is clear that the relatively infrequent sampling by the drifter makes any interpretation tentative. In 1987, the species composition was dominated by large centric diatoms, along with *Chaetoceros* in the nearshore waters. The large centric diatoms increased in volume and relative abundance as the drifter moved offshore. In 1988, the species composition shifted from *Chaetoceros* to *Rhizosolenia* to dinoflagellates as the drifter moved offshore, with large centric diatoms forming a relatively constant background.

Figure 7 shows a spline fit to the drifter positions in 1988 compared with the geopotential anomaly [Huyer *et al.*, 1991]. When compared with a similar figure from the 1987 deployment (Fig. 4, Abbott *et al.* [1990]), it is apparent that the 1988 deployment more nearly sampled the core of the meander. In 1987, the drifter tended to be inshore of the high velocity portion of the meander. The jet appears to have been stronger in 1988, based on estimates of the geopotential anomaly [Huyer *et al.*, 1991; Kosro *et al.*, 1991]. In the Point Arena region, the filament was much narrower and more sharply defined than it was in 1987. Although both deployments sampled regions of considerable variability, it appears (based on both the fluorescence and species data) that there was more heterogeneity in 1988 along the core of the meander.

3.3 Estimates of Primary Productivity

Although we recognize that there are inherent errors in the sun-stimulated fluorescence measurements that result from changes in the light utilization characteristics of the phytoplankton we have estimated primary productivity (Figure 9) using the model proposed by Kiefer *et al.* [1989] and Chamberlin *et al.* [1990]. In 1987 (Figure 9a), primary productivity was surprisingly uniform along the drifter track, compared with the more intense variability in chlorophyll (Figure 3). It decreased by only a factor of two from the beginning to the end of the deployment whereas chlorophyll decreased by a factor of four. In comparison, the pattern of productivity was much more variable as the drifter moved offshore in 1988 (Figure 9b), decreasing from 150 to 30 ng-at C m⁻³ s⁻¹. This variability is largely driven by the variations in chlorophyll, which were also much larger than in 1987.

The productivity:chlorophyll biomass ratio (P^B) is shown in Figure 10. Clearly, this ratio was much higher in 1987 than in 1988. Even nearshore where chlorophyll values were relatively high in both years, phytoplankton were growing more rapidly on a per unit biomass basis in 1987 by a factor of five to ten (Figure 10a). However, it should be noted that there are numerous assumptions in the productivity and chlorophyll calculations that could cause these estimates to be in error. We compared our P^B estimates in 1987 with those of Hood *et al.* [1991] who used direct C¹⁴ measurements. Although Hood *et al.* [1991] sampled at somewhat different locations and times in 1987, the range of P^B is about the same, accounting for changes in units. Chavez *et al.* [1991] published maps of integrated chlorophyll and estimates of primary productivity (from a regression model of PAR and chlorophyll) for 1988. While these are not directly comparable to our estimates of near-surface P^B, the change from

nearshore to offshore was from about 4 to 30 in *Chavez et al.* [1991], a relative nearshore/offshore increase similar to that shown in Figure 10b. Thus the patterns of relative changes in P^B are reasonable.

In 1987, we note that P^B was lower on day 169, when chlorophyll was at its highest. P^B was also low on part of day 171 when chlorophyll levels again increased. This suggests that the changes in P^B were dominated by changes in chlorophyll content in 1987. However, the general pattern is for P^B to increase as the drifter moves offshore. In 1988, the pattern is much less variable (in contrast to the productivity and chlorophyll values in Figure 9b and Figure 5). As noted above, the drifter in 1988 more nearly followed the core of the much stronger meander whereas in 1987 the drifter stayed inshore of the weaker meander. Even offshore where chlorophyll values were nearly the same in both years, P^B was much higher in 1987. This is consistent with the general pattern where there is higher absolute productivity in the freshly upwelled water in the core of the meander and lower productivity offshore or in places or years where the meander is weaker. The patterns of P^B , however, are the reverse. A similar pattern was noted by *Hood et al.* [1991]; the highest primary productivity rates were inshore of the meandering jet. As noted earlier, the differences in species composition between 1987 and 1988 were likely an important element of the interannual differences in P^B .

Using the beam transmission data, we estimated primary productivity following the methods described by *Siegel et al.* [1989]. Clearly, there are numerous assumptions in this method, but we wished to compare the relative magnitudes and patterns of these two approaches. Table 1 shows the values for both the sun-stimulated fluorescence and beam attenuation methods. Although the two estimates do not agree exactly, the patterns and magnitude of change are similar as the drifter moved offshore. However, it is clear that both the beam attenuation and sun-stimulated fluorescence estimates are fraught with difficulties. The fact that they are similar may simply be happenstance. On a daily basis, however, we think that these estimates can be used to evaluate relative changes in productivity and biomass.

Stramska and Dickey [1992] note that the bio-optical properties of phytoplankton can change rapidly on diel scales, thereby confounding simple interpretation of beam attenuation and fluorescence in terms of either chlorophyll biomass or primary productivity. We thus plotted the ratio of beam attenuation to strobe fluorescence from 1987 as a function of PAR as in Figure 17 of *Stramska and Dickey* [1992]. Figure 11 shows the nearshore (days 168–171) and offshore (days 172–176) data. These are quite similar to the 10 m data from *Stramska and Dickey* [1992], which suggests that much of the diel variation is caused by changes in the bio-optical properties of the phytoplankton. In particular, changes in cellular chlorophyll may change both fluorescence and beam attenuation in parallel during the daylight hours. As with *Stramska and Dickey* [1992], we note no apparent quenching of fluorescence by PAR. The offset between the inshore waters and the offshore waters implies that there was more scattering and absorption offshore per unit of fluorescence (chlorophyll), as noted by *Abbott et al.* [1990].

3.4 Small-scale Variability

A general picture emerges from the two drifter deployments. Changes in the strength of the meander correspond with changes in species composition, primary productivity, and P^B . Biomass and primary productivity decrease offshore as nutrients become depleted, but P^B increases. Phytoplankton become more strongly scattering per unit chlorophyll in offshore waters. Thus the meander represents a sharp demarcation between both the biological and bio-optical properties of the phytoplankton. Physical processes such as upwelling and downwelling along the meander play an important role in the smaller scale variability of these properties.

To examine these small-scale patterns, we calculated variance spectra from several of the physical and bio-optical time series. We analyzed only those time series where there was a continuous record (temperature, beam attenuation, and strobe fluorescence). We used maximum entropy methods (MEM) to calculate the spectra; as we limited our discussion to time scales greater than five hours, this method should not produce spurious results. Comparison with structure functions showed that the MEM spectra captured the same scales of variability at these longer time scales. We varied the number of poles used to calculate the MEM spectra as well; we used these results to estimate the minimum period that could be reasonably studied based on the robustness of the various spectral peaks. In our case, periods less than five hours showed considerable variability in the number of peaks as a function of the number of poles used in the calculation.

Figure 12 shows a typical MEM spectrum, in this case beam attenuation from the 1987 record. A strong peak is present with a period of 24 hours with smaller peaks at 16, 12, 8, and 6 hours. Temperature and especially strobe fluorescence show similar diurnal and semi-diurnal peaks. The diurnal signal has been noted in many other bio-optical records [*Dickey et al.*, 1993; *Stramska and Dickey*, 1992; *Dickey et al.*, 1991]. In the case of strobe fluorescence, diel variability is the result of the changes in fluorescence response to changes in solar irradiance [*Kiefer*, 1973; *Stramska and Dickey*, 1992]. For temperature, diel variability is also the result of changes in solar irradiance which causes near-surface heating during the day and is visible in the offshore portions of the deployments in both years. Beam attenuation is thought to change as a result of both growth in the number of particles as well as changes in their scattering properties [*Siegel et al.*, 1989; *Cullen et al.*, 1992; *Stramska and Dickey*, 1992]. A peak at the semi-diurnal period has not been observed in other bio-optical time series [*Dickey et al.*, 1991] which have strong diurnal signals, but it is quite pronounced in the strobe fluorescence data from the 1987 deployment (Figure 13). Smaller peaks were visible in the temperature and beam attenuation spectra at the semi-diurnal period. A semi-diurnal tide may be the cause of this peak, similar to the semi-diurnal peaks found in current meter records off northern California [*Noble et al.*, 1987; *Rosenfeld and Beardley*, 1987]. This could result in water motions which would change the bio-optical and temperature properties of the water at the drifter. Fluorescence could change either as the result of changes in chlorophyll content or as a photoadaptive response to changing light levels as deeper water is brought closer to the surface. Although the

strong diurnal signal could result in an overtone to appear at the semi-diurnal frequency, note that no such overtone appears in the 1988 fluorescence spectrum

The patterns of variance appear to differ between nearshore and offshore, so we divided each deployment time series in half. Thus we considered days 168–172 from 1987 and 186–189 from 1988 as the nearshore time series and days 172–176 from 1987 and 189–192 from 1988 as the offshore time series. We passed each time series through a band reject filter, removing the strong diurnal signal from all variables. For strobe fluorescence, we removed both the diurnal and semi-diurnal signals. Figure 14 shows the MEM spectrum for temperature from both deployments. Although the level of variance is different between the two deployments in the nearshore region, the slopes are nearly identical (about -2). A peak is visible at ten hours in 1987 (Figure 14a) but in general neither nearshore spectrum shows much structure. The nearshore spectrum of beam attenuation (Figure 15) is flatter than the nearshore temperature spectrum from 1987 (Figure 14a) with a slope of about -1.5 and a peak at 15 hours rather than at 10 hours. The shapes of the nearshore strobe fluorescence spectra (Figure 16) are slightly different with a slope of -2 in 1987 and -1.5 in 1988. There is a noticeable semi-diurnal peak in 1987 (Figure 16a). Despite these subtle differences, the nearshore spectra of all three variables are generally similar in their lack of strong peaks. This is most likely a result of the intense, mesoscale variability present in the nearshore region that occurs over a continuum of time scales.

The offshore variance spectra behave much more irregularly. Figure 14 shows the spectra for temperature from the offshore regions in 1987 and 1988. As with the nearshore series, both data sets were passed through a band reject filter to remove the diurnal signal. In 1987 (Figure 14a), the spectrum is dominated by much stronger peaks at 19, 6 and 3 hours than nearshore. In contrast, the 1988 temperature spectrum (Figure 14b) was dominated by a peak near 20 hours. The bio-optical variables also varied in a less continuous manner offshore. Beam attenuation (Figure 15) is dominated by distinct peaks at 48, 20, and 7 hours. Strobe fluorescence (Figure 16) has a peak at 19 hours in both 1987 and 1988, although it is more pronounced in the second year along with a peak at 8 hours in 1988 (Figure 16b) and at 6.5 hours in 1987. Given the lower level of variability in the offshore regions, it is not surprising to see the variance spectra dominated by distinct periods. We have no explanation for the peaks that occur in the 6–8 hour range. They may be caused by internal waves which are propagating past the drifter. Of more interest is the consistent peak in the 19–20 hour range.

As the inertial period at this latitude (39°N) is a little over 19 hours, we suspect that the drifter was being subjected to organized inertial motions in the offshore region, similar to those noted by *Paduan and Niiler* [1990] in the CTZ region. These organized motions may have moved the drifter along a front in bio-optical properties as well as temperature. We note that the strength of the inertial peak is much larger in 1988 in both temperature and strobe fluorescence when the drifter was nearly in the core of the meandering jet. As noted by *Paduan and Niiler* [1990] and *Swenson et al.* [1992], the jet is nearly geostrophic in the offshore domain, and there are strong inertial features in the drifter tracks. *Paduan and Niiler* [1990]

calculated a horizontal scale of about 3 km for these features. *Swenson et al.* [1992], examining similar scales of motion, estimated vertical motions of 10–20 m/day that were associated with these features. These vertical motions, caused by changes in relative vorticity, are similar to those described for a front in the Sargasso Sea by *Pollard and Regier* [1992]. These strong vertical motions are likely to have a strong effect on the bio-optical properties observed by the drifter package.

We tested the performance of our band reject filter with time series composed of sinusoid functions contaminated by random noise. The filter successfully removed the desired frequencies so we do not think that the 19–20 hour peak is some artifact caused by the removal of the 24-hour signal.

The presence of intense vertical motions along the drifter path, either through subduction processes [*Kadko et al.*, 1991; *Washburn et al.*, 1991] or through vorticity adjustments caused by inertial motions, obviously complicates the interpretation of the drifter data. As noted earlier, phytoplankton species composition changes considerably in association with changes in the direction of vertical motion. However, we are able to interpret the patterns of temporal change in terms of changes in the physical circulation field. While we cannot assume that the drifter is truly following a patch of phytoplankton, these data show the influence of inertial and tidal motions on bio-optical properties as well as the larger scale changes that occur between nearshore and offshore.

4. SUMMARY AND CONCLUSIONS

The two deployments of a bio-optical drifter in the coastal transition zone off northern California were analyzed in terms of the performance of several bio-optical algorithms and in terms of large and small-scale variability. With the availability of long-term bio-optical sampling, we need to understand the limits and advantages of these data sets. Bio-optical relationships can change dramatically on a wide range of time and length scales, thus complicating any analysis.

The general features of the waters off northern California were similar in the two years. Chlorophyll, particulate concentration, and primary productivity were higher and more variable in the nearshore waters than offshore. P^B and scattering per unit chlorophyll, however, were lower nearshore and higher offshore. The separation between nearshore and offshore properties was delineated by the meandering jet, which separated distinct phytoplankton communities based on species counts. Similar distinctions were noted by *Hood et al.* [1991] and *Chavez et al.* [1991] for the coastal transition zone region. There were significant changes in species composition (and size structure of the community) both along the drifter tracks and between the two deployments. Although the phytoplankton sampling ceased to operate in the far offshore waters, other observations showed that this region was dominated by small forms, primarily flagellates [*Hood et al.*, 1991].

We applied several methods to estimate chlorophyll, using downwelling irradiance ratios [*Smith et al.*, 1991], beam attenuation [*Siegel et al.*, 1989], sun-stimulated fluorescence [*Chamberlin et al.*, 1990], and conventional strobe fluorescence. Although the general patterns were similar (high, variable chloro-

phyll values nearshore, decreasing rapidly as the drifter moved offshore), there was considerable difference in the detailed structure of the time series. The relationship between chlorophyll derived from strobe fluorescence and that derived from sun-stimulated fluorescence differed considerably between 1987 and 1988. In the latter deployment, a different set of coefficients for sun-stimulated fluorescence was required to obtain agreement between the two fluorescence estimates, and these coefficients needed to be altered along the drifter track as it moved from nearshore to offshore. It appeared that strong changes in the phytoplankton community were largely responsible for the changes in the fluorescence relationships. The beam attenuation data were available only during the first deployment, but they revealed strong onshore/offshore differences in bio-optical properties, especially in the amount of scattering per unit chlorophyll.

We examined small-scale variability through variance spectral analysis. A strong diel signal was present in many of the bio-optical variables, as expected. In particular, strobe fluorescence showed a consistent pattern in relation to the amount of solar radiation. Beam attenuation showed a similar diel pattern in the offshore waters. We suggest that this is the result of grazing activity but changes in the optical properties of phytoplankton would cause a similar pattern. A semi-diurnal signal was present in temperature and strobe fluorescence and is perhaps related to the semi-diurnal tide. An unexpected peak was found at the inertial period (19 hours) in the bio-optical variables and in temperature. This peak, however, was present only in the offshore waters in both 1987 and 1988. Organized inertial motions of the drifter in the offshore portion of the meander have been observed in other drifter data sets from northern California. These inertial motions are sometimes associated with strong vertical motions caused by changes in relative vorticity. The bio-optical properties varied in response either to these vertical motions or to changes in the relative horizontal position of the drifter as it moved along the meander.

The proximate cause in the temporal and spatial changes was variability in phytoplankton species composition. Such species-dependence has been noted in many studies and is not unexpected. The ultimate cause, however, appears to be changes in the physical environment. For example, the strength of the meander as well as distance from the meander appeared to affect the phytoplankton species composition. Similarly, vertical velocities associated with organized inertial motions in the offshore region result in a pronounced bio-optical response. Similar questions were raised about fluorometric methods when they were introduced nearly 30 years ago. Many of the problems were addressed simply by more frequent calibration samples. However, it is clear that such calibration sampling must be done on a scale appropriate for the inherent variability in the process under study. Unfortunately, we know little about these scales in the biological realm. Of more concern is the recent availability of unattended sampling devices where calibration sampling is not possible. Analysis of such data must be conducted with the awareness that variability in the relationships of interest (such as beam attenuation and particulate abundance) will have its own temporal and spatial scales. However, we now have some information on the temporal and spatial scales of variability that will be useful in future data assimilation models. Future work

must extend these observations over a broad range of physical and biological conditions as it is apparent that the scales of variability can change dramatically.

Acknowledgments. We thank P. Niiler for providing the drifters and assisting with design and deployment. We thank R. Hood for design and construction of the drifter packages for the second deployment. G. Friederich provided technical assistance for the water sampler. R. Limeburner and T. Cowles assisted with deployments. B. Barksdale assisted with programming and data analysis. This work was supported by the Office of Naval Research (grants to M.R.A. and K.H.B.) and by the National Aeronautics and Space Administration (grants to M.R.A. and C.O.D.).

REFERENCES

- Abbott, M. R., Phytoplankton patchiness: ecological implications and observation methods, in *Patchiness in Terrestrial and Marine Systems*, edited by S. A. Levin, T. M. Powell, and J. H. Steele, pp. 37-49, Springer-Verlag, New York, 1993.
- Abbott, M. R., K. H. Brink, C. R. Booth, D. Blasco, L. A. Codispoti, P. P. Niiler, and S. R. Ramp, Observations of phytoplankton and nutrients from a Lagrangian drifter off northern California, *J. Geophys. Res.*, **95**, 9393-9409, 1990.
- Bartz, R., R. V. Zaneveld, and H. Pak, A transmissometer for profiling and moored observations in water, *Proc. Soc. Photo. Opt. Eng.*, **160**, 102-108, 1978.
- Bishop, J. K. B., The correction and suspended material calibration of Sea Tech transmissometer data, *Deep Sea Res.*, **33**, 121-134, 1986.
- Bricaud, A., A.-L. Bedhomme, and A. Morel, Optical properties of diverse phytoplanktonic species: Experimental results and theoretical interpretation, *J. Plankton Res.*, **10**, 851-873, 1988.
- Brink, K. H., and T. J. Cowles, The coastal transition zone program, *J. Geophys. Res.*, **96**, 14,637-14,647, 1991.
- Brink, K. H., R. C. Beardsley, P. P. Niiler, M. Abbott, A. Huyer, S. Ramp, T. Stanton, and D. Stuart, Statistical properties of near surface flow in the California coastal transition zone, *J. Geophys. Res.*, **96**, 14,693-14,706, 1991.
- Bryan, F., Parameter sensitivity of primitive equation ocean general circulation models, *J. Phys. Oceanogr.*, **17**, 970-985, 1987.
- Chamberlin, W. S., C. R. Booth, D. A. Kiefer, J. H. Morrow, and R. C. Murphy, Evidence for a simple relationship between natural fluorescence, photosynthesis, and chlorophyll in the sea, *Deep Sea Res.*, **37**, 951-973, 1990.
- Chavez, F. P., R. T. Barber, P. M. Kosro, A. Huyer, S. R. Ramp, T. P. Stanton, and B. Rojas de Mendiola, Horizontal transport and the distribution of nutrients in the coastal transition zone off northern California: Effects on primary production, phytoplankton biomass and species composition, *J. Geophys. Res.*, **96**, 14,833-14,848, 1991.
- Chelton, D. B., and M. G. Schlax, Estimation of time-averages from irregularly spaced observations: With application to coastal zone color scanner estimates of chlorophyll concentration, *J. Geophys. Res.*, **96**, 14,669-14,692, 1991.
- Collins, D. J., C. R. Booth, C. O. Davis, D. A. Kiefer, and C. Stallings, A model of the photosynthetically available and usable irradiance in the sea, *SPIE Ocean Optics IX*, **925**, 87-100, 1988.
- Cullen, J. J., M. R. Lewis, C. O. Davis, and R. T. Barber, Photosynthetic characteristics and estimated growth rates indicate grazing is the proximate control of primary production in the equatorial Pacific, *J. Geophys. Res.*, **97**, 639-654, 1992.
- Denman, K. L., and H. J. Freeland, Correlation scales, objective mapping and a statistical test of geostrophy over the continental shelf, *J. Mar. Res.*, **43**, 517-539, 1985.
- Denman, K. L., and T. M. Powell, Effects of physical processes on planktonic ecosystems in the coastal ocean, *Oceanogr. Mar. Biol. Ann. Rev.*, **22**, 125-168, 1984.
- Dickey, T. D., The emergence of concurrent high-resolution physical and bio-optical measurements in the upper ocean and their applica-

- tions, *Rev. Geophys.*, 29, 383-413, 1991.
- Dickey, T. D., J. Marra, T. Granata, C. Langdon, M. Hamilton, J. Wiggert, D. Siegel, and A. Bratkovich, Concurrent high resolution bio-optical and physical time series observations in the Sargasso Sea during the spring of 1987, *J. Geophys. Res.*, 96, 8643-8663, 1991.
- Dickey, T. D., T. Granata, J. Marra, C. Langdon, J. Wiggert, Z. Chai-Jochner, M. Hamilton, J. Vazquez, M. Stramska, R. Bidigare, and D. Siegel, Seasonal variability of bio-optical and physical properties in the Sargasso Sea, *J. Geophys. Res.*, 98, 865-898, 1993.
- Falkowski, P., and D. A. Kiefer, Chlorophyll *a* fluorescence in phytoplankton: Relationship to photosynthesis and biomass, *J. Plankton Res.*, 7, 715-731, 1985.
- Friederich, G. E., P. J. Kelly, and L. A. Codispoti, An inexpensive moored water sampler for investigating chemical variability, in *Tidal Mixing and Plankton Dynamics*, edited by M. J. Bowman, C. M. Yentsch, and W. T. Peterson, pp. 463-482, Springer-Verlag, New York, 1986.
- Gordon, H. R., D. K. Clark, J. W. Brown, O. B. Brown, R. H. Evans, and W. W. Broenkow, Phytoplankton pigment concentrations in the Middle Atlantic Bight: Comparison between ship determinations and coastal zone color scanner estimates, *Appl. Optics*, 22, 20-36, 1983.
- Gordon, H. R., O. B. Brown, R. H. Evans, J. W. Brown, R. C. Smith, K. S. Baker, and D. K. Clark, A semianalytic radiance model of ocean color, *J. Geophys. Res.*, 93, 10,909-10,924, 1988.
- Harris, G. P., *Phytoplankton Ecology: Structure, Function, and Fluctuation*, 384 pp., Chapman and Hall, New York, 1986.
- Hood, R., M. R. Abbott, P. M. Kosro, and A. Huyer, Relationships between physical structure and biological pattern in the surface layer of a northern California upwelling system, *J. Geophys. Res.*, 95, 18,081-18,094, 1990.
- Hood, R., M. R. Abbott, and A. E. Huyer, Phytoplankton and photosynthetic light response in the coastal transition zone off northern California in June 1987, *J. Geophys. Res.*, 96, 14,769-14,780, 1991.
- Huyer, A., P. M. Kosro, J. Fleischbein, S. R. Ramp, T. Stanton, L. Washburn, F. P. Chavez, T. J. Cowles, S. D. Pierce, and R. L. Smith, Currents and water masses of the coastal transition zone off northern California, June to August 1988, *J. Geophys. Res.*, 96, 14,809-14,831, 1991.
- Kadko, D. C., L. Washburn, and B. Jones, Evidence of subduction within cold filaments of the northern California coastal transition zone, *J. Geophys. Res.*, 96, 14,909-14,926, 1991.
- Kiefer, D. A., Chlorophyll *a* fluorescence in marine centric diatoms: Responses of chloroplasts to light and nutrients, *Mar. Biol.*, 23, 39-45, 1973.
- Kiefer, D. A., W. S. Chamberlin, and C. R. Booth, Natural fluorescence of chlorophyll *a*: Relationship to photosynthesis and chlorophyll concentration in the western South Pacific gyre, *Limnol. Oceanogr.*, 34, 868-881, 1989.
- Kirk, J. T. O., *Light and Photosynthesis in Aquatic Ecosystems*, 401 pp., Cambridge University Press, Cambridge, England, 1983.
- Kishino, M., S. Sugihara, and N. Okami, Estimation of quantum yield of chlorophyll *a* fluorescence from the upward irradiance spectrum in the sea, *La Mer*, 22, 233-240, 1984.
- Kosro, P. M., A. Huyer, S. R. Ramp, R. L. Smith, F. P. Chavez, T. J. Cowles, M. R. Abbott, P. T. Strub, R. T. Barber, P. F. Jensen, and L. F. Small, The structure of the transition zone between coastal waters and the open ocean off northern California, winter and spring 1987, *J. Geophys. Res.*, 96, 14,707-14,730, 1991.
- Morel, A., and A. Bricaud, Theoretical results concerning light absorption in a discrete medium, and application to specific absorption of phytoplankton, *Deep Sea Res.*, 28, 1375-1393, 1981.
- Niiler, P. P., R. E. Davis, and H. J. White, Water-following characteristics of a mixed layer drifter, *Deep Sea Res.*, 34, 1867-1881, 1987.
- Noble, M., L. K. Rosenfeld, R. L. Smith, J. V. Gardner, and R. C. Beardsley, Tidal currents seaward of the northern California continental shelf, *J. Geophys. Res.*, 92, 1733-1744, 1987.
- Paduan, J. D., and P. P. Niiler, A Lagrangian description of motion in northern California coastal transition filaments, *J. Geophys. Res.*, 95, 18,095-18,110, 1990.
- Pollard, R. T., and L. A. Regier, Vorticity and vertical circulation at an ocean front, *J. Phys. Oceanogr.*, 22, 609-625, 1992.
- Rosenfeld, L. K., and R. C. Beardsley, Barotropic semi-diurnal tidal currents off northern California during the Coastal Ocean Dynamics Experiment (CODE), *J. Geophys. Res.*, 92, 1721-1732, 1987.
- Siegel, D. A., T. D. Dickey, L. Washburn, M. K. Hamilton, and B. G. Mitchell, Optical determination of particle abundance and production variations in the oligotrophic ocean, *Deep Sea Res.*, 36, 211-222, 1989.
- Smith, R. C., K. J. Waters, and K. S. Baker, Optical variability and pigment biomass in the Sargasso Sea as determined using deep-sea optical mooring data, *J. Geophys. Res.*, 96, 8665-8686, 1991.
- Stegmann, P. M., M. R. Lewis, C. O. Davis, and J. J. Cullen, Primary production estimates from recordings of solar-stimulated fluorescence in the equatorial Pacific at 150°W, *J. Geophys. Res.*, 97, 627-638, 1992.
- Stramska, M., and T. D. Dickey, Variability of bio-optical properties of the upper ocean associated with diel cycles in phytoplankton population, *J. Geophys. Res.*, 97, 17,873-17,887, 1992.
- Strub, P. T., et al., The nature of the cold filaments in the California Current system, *J. Geophys. Res.*, 96, 14,743-14,768, 1991.
- Swenson, M. S., P. P. Niiler, K. H. Brink, and M. R. Abbott, Drifter observations of a cold filament off Point Arena, California, in July 1988, *J. Geophys. Res.*, 97, 3593-3610, 1992.
- Washburn L., D. C. Kadko, B. H. Jones, T. Hayward, P. M. Kosro, T. P. Stanton, S. Ramp, and T. Cowles, Water mass subduction and the transport of phytoplankton in a coastal upwelling system, *J. Geophys. Res.*, 96, 14,927-14,945, 1991.
- Zaneveld, J. R. V., An asymptotic closure theory for irradiance in the sea and its inversion to obtain the inherent optical properties, *Limnol. Oceanogr.*, 34, 1442-1452, 1989.
- M. R. Abbott, College of Oceanic and Atmospheric Sciences, Oregon State University, Corvallis, OR 97331-5503.
- K. H. Brink, Woods Hole Oceanographic Institution, Woods Hole, MA 02543.
- C. R. Booth, Biospherical Instruments, Inc., 5340 Riley Street, San Diego, CA 92110-2621.
- D. Blasco, 102 De Sept Lacs, St. Donat, Rimouski, Québec, Canada G0K 1L0.
- M. S. Swenson, Atlantic Oceanographic and Meteorological Laboratory, National Oceanic and Atmospheric Administration, 4301 Rick-enbacker Causeway, Miami, FL 33149.
- C. O. Davis, Jet Propulsion Laboratory, California Institute of Technology, 4800 Oak Grove Drive, Pasadena, CA 91109.
- L. A. Codispoti, Office of Naval Research, Code 3241, 800 N. Quincy St., Arlington, VA 22217-5660.

(Received xxxxxxx;
revised xxxxxx;
accepted xxxxxxx.)

¹College of Oceanic and Atmospheric Sciences, Oregon State University, Corvallis.

²Woods Hole Oceanographic Institution, Woods Hole, Massachusetts.

³Biospherical Instruments, Incorporated, San Diego, California.

⁴Québec, Canada.

⁵Atlantic Oceanographic and Meteorological Laboratory, National Oceanic and Atmospheric Administration, Miami, Florida.

⁶Jet Propulsion Laboratory, California Institute of Technology, Pasadena.

⁷Office of Naval Research, Arlington, Virginia.

Copyright 19xx by the American Geophysical Union.

Paper number 9xxxxxxx.
xxxx-xxxx/xx/xxXX-xxxxx\$0x.xx

Fig. 1. (a) Drifter path from 1987 superimposed over AVHRR image of sea surface temperature from Abbott et al. [1990]. (b) Drifter path from 1988 superimposed over AVHRR image of sea surface temperature.

Fig. 2. (a) Time series of temperature ($^{\circ}\text{C}$) from the 1988 deployment. (b) Same as a but for strobe fluorescence. (c) Same as a but for photosynthetically available radiation ($\mu\text{Ein}/\text{m}^2/\text{s}^1$).

Fig. 3. Estimates of chlorophyll (mg/m^3) using four data sets from the 1987 deployment. Observations are constrained to between 1100 and 1500 h local time for each day, and they are plotted successively without time gaps.

Fig. 4. Estimates of phytoplankton backscatter (m^{-1}) using two algorithms for the 1987 deployment. Observations are constrained to between 1100 and 1500 h local time.

Fig. 5. Estimates of chlorophyll (mg/m^3) using three data sets from the 1988 deployment. Observations are constrained to between 1100 and 1500 h local time. The Kishino/Collins parameters (0.04, 0.045 model) for the sun-stimulated fluorescence estimates are compared with the Chamberlin parameters (0.016, 0.028 model).

Fig. 6. Relative phytoplankton species abundance from the 1988 deployment in terms of % total cell volume.

Fig. 7. Path of 1988 drifter overlain on geopotential anomaly from the 6–12 July cruise (year days 188–194). Geopotential anomaly is from Huyer et al. [1991] and is calculated at 50 dbar relative to 500 dbar.

Fig. 8. (a) Horizontal section of chlorophyll from vertical profiles collected at approximately noon each day next to the drifter in 1988. Date and location of each profile are marked at the top. (b) Same as a but for temperature. (c) Same as a but for salinity.

Fig. 9. (a) Estimates of instantaneous primary productivity ($\text{ng-at C}/\text{m}^3/\text{s}$) based on sun-stimulated fluorescence from the 1987 deployment. Observations are constrained to between 1100 and 1500 h local time. (b) Same as a except from the 1988 deployment.

Fig. 10. (a) Productivity per unit chlorophyll (P^B) from the 1987 deployment. (b) Same as a except from the 1988 deployment.

Fig. 11. Beam attenuation coefficient versus strobe fluorescence from the 1987 deployment.

Fig. 12. Variance spectrum derived using the maximum entropy method for beam attenuation from the 1987 deployment.

Fig. 13. Same as Fig. 12 except for strobe fluorescence.

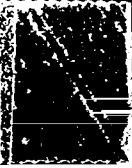
Fig. 14. (a) Variance spectrum for temperature from the 1987 deployment. Data were passed through a band-reject filter, removing the 24 hour cycle. (b) Same as a except from the 1988 deployment.

Fig. 15. Variance spectrum for beam attenuation from the 1987 deployment. Data were passed through a band-reject filter, removing the 24 hour cycle.

Fig. 16. (a) Variance spectrum for strobe fluorescence from the 1987 deployment. Data were passed through a band-reject filter, removing the 12 and 24 hour cycles. (b) Same as a except from the 1988 deployment.

TABLE 1. Estimates of primary productivity ($\text{mg-at C m}^{-3} \text{ hr}^{-1}$) using beam attenuation and sun-stimulated fluorescence models. No beam attenuation estimate was available for Day 171 because beam attenuation decreased during the day.

	Beam Attenuation	Sun-stimulated Fluorescence
Day 169	0.17	0.16
Day 170	0.20	0.17
Day 171	n/a	0.14
Day 172	0.08	0.14
Day 173	0.06	0.11
Day 174	0.07	0.11
Day 175	0.09	0.10



22 JUN 87

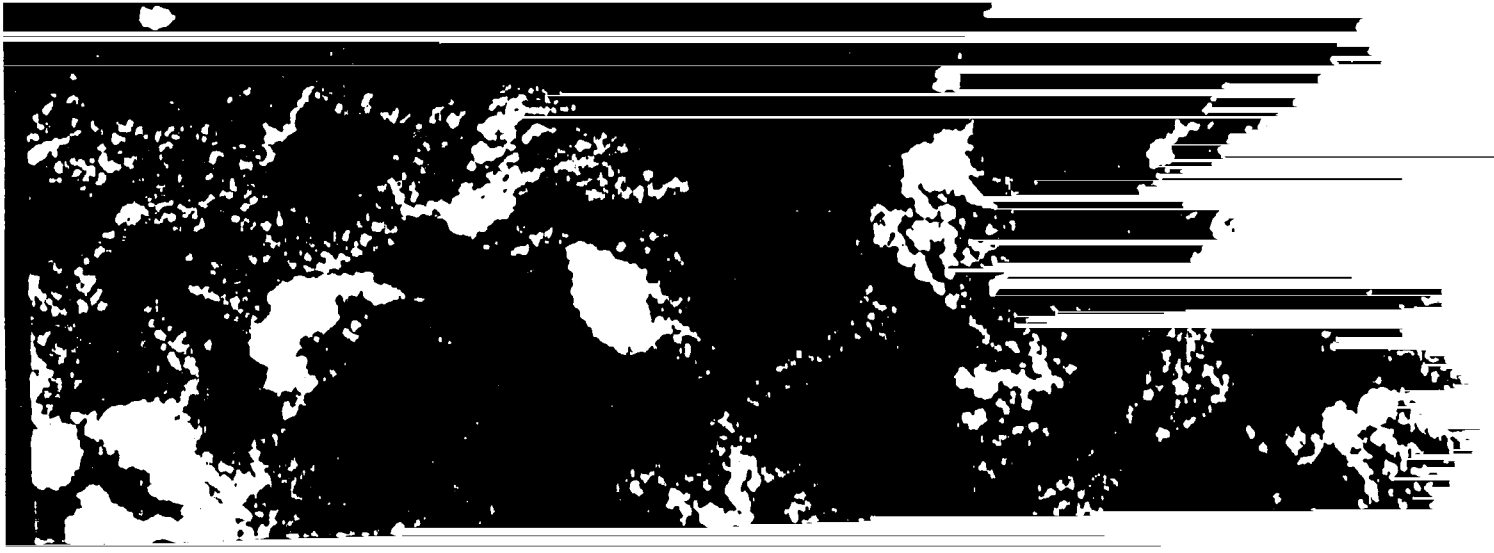
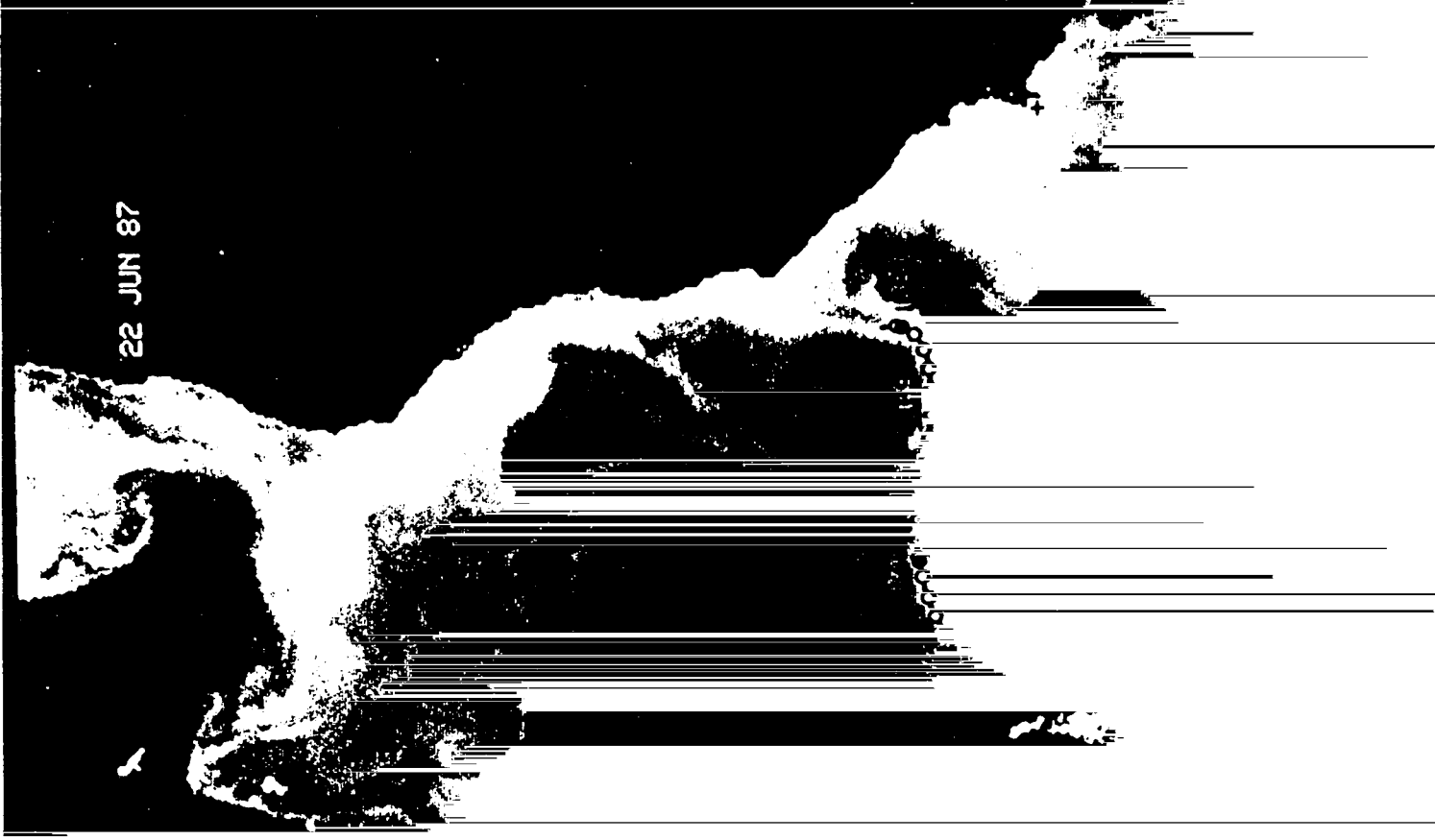
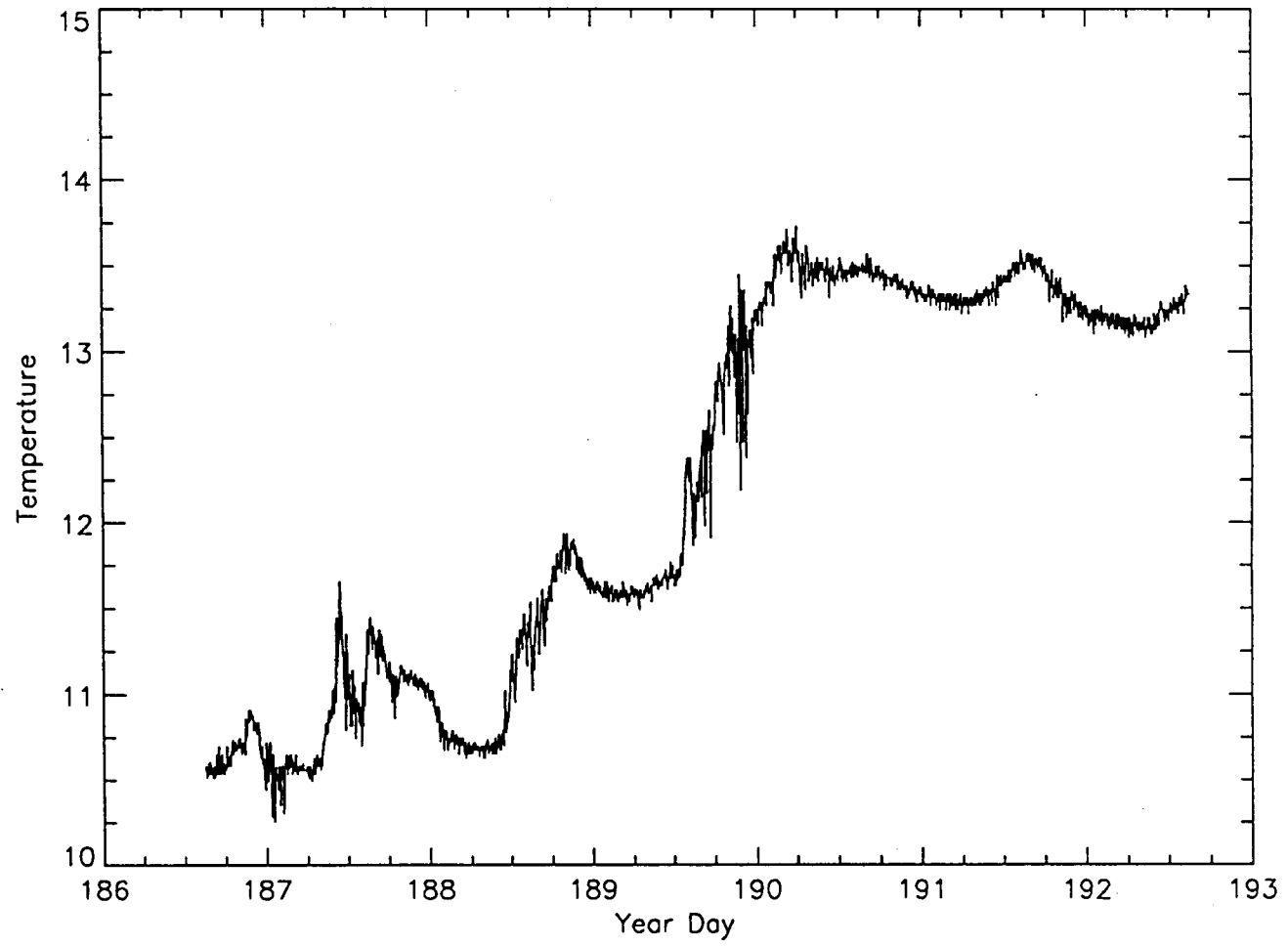


Fig. 1B



Fig. 2A



Sts. 2B

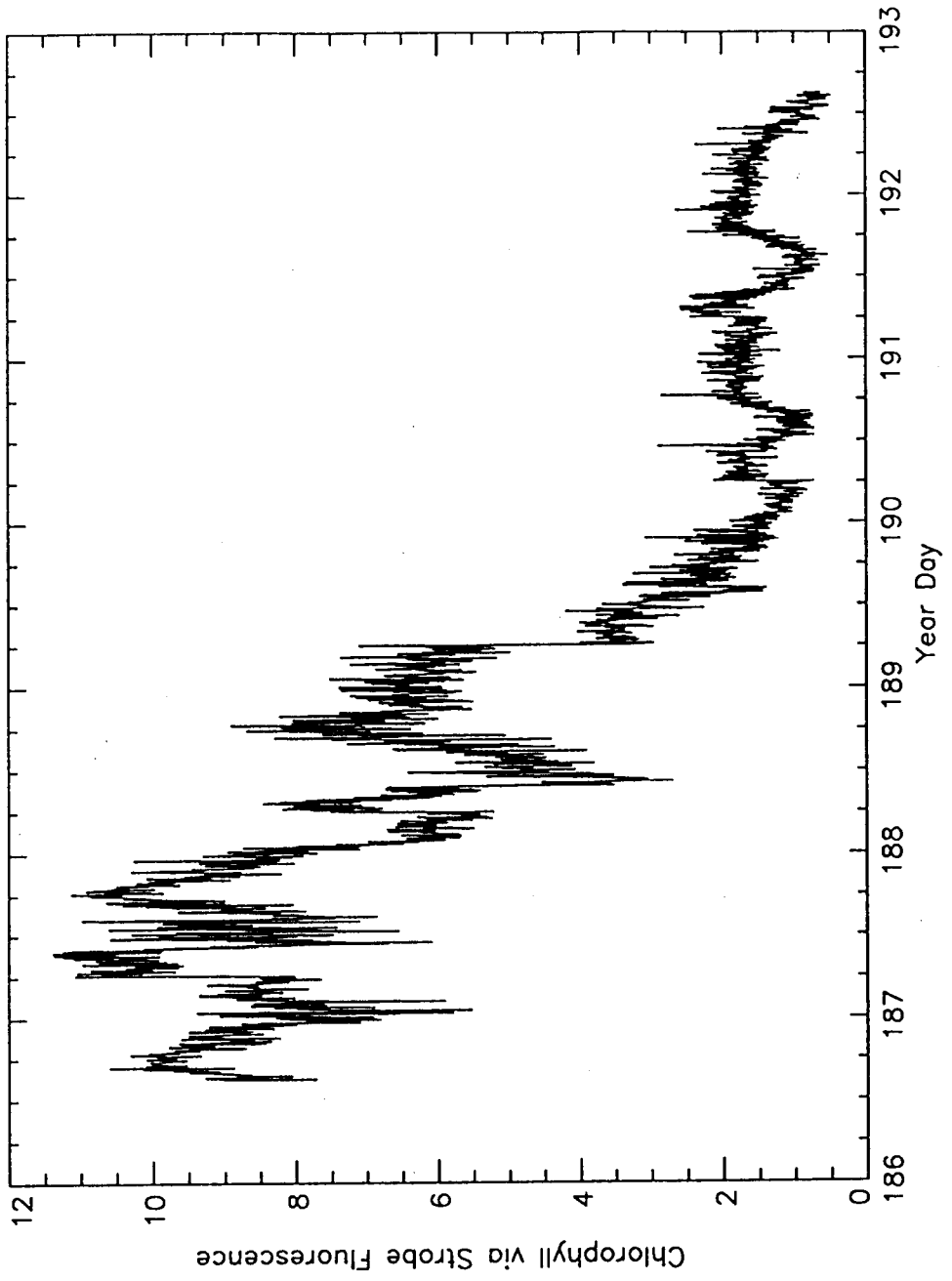


Fig. 2c

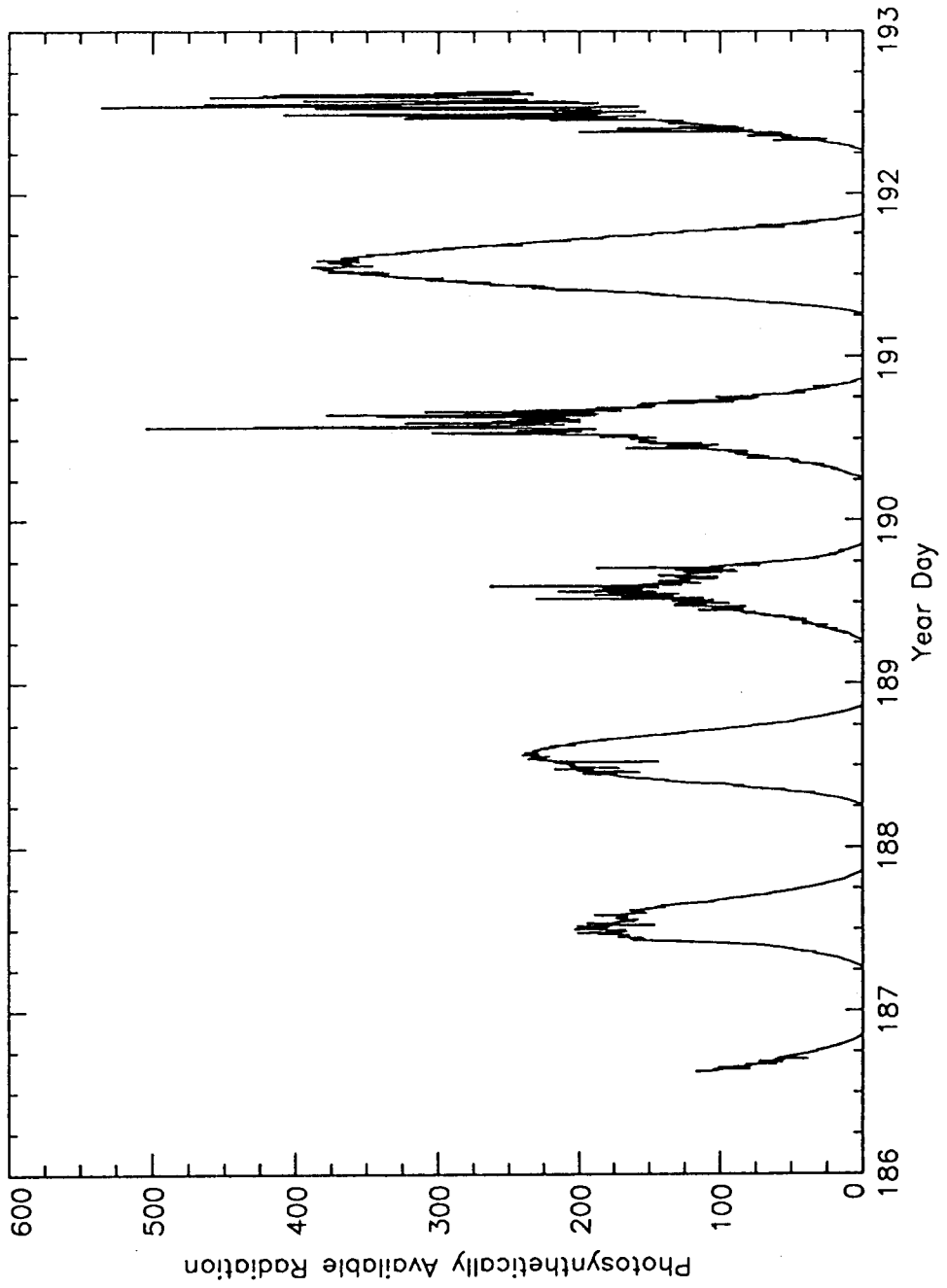


Fig. 3

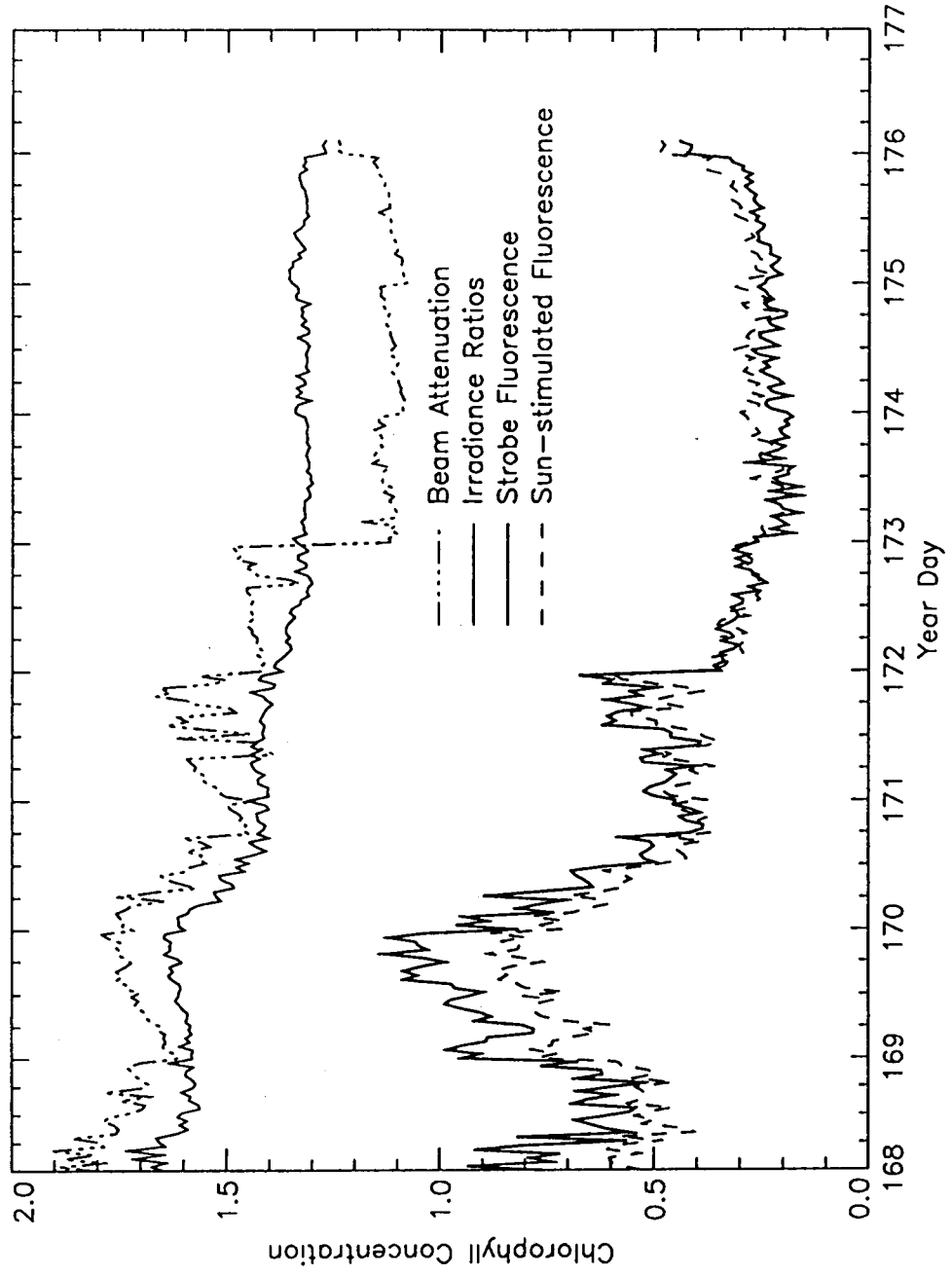


Fig. 4

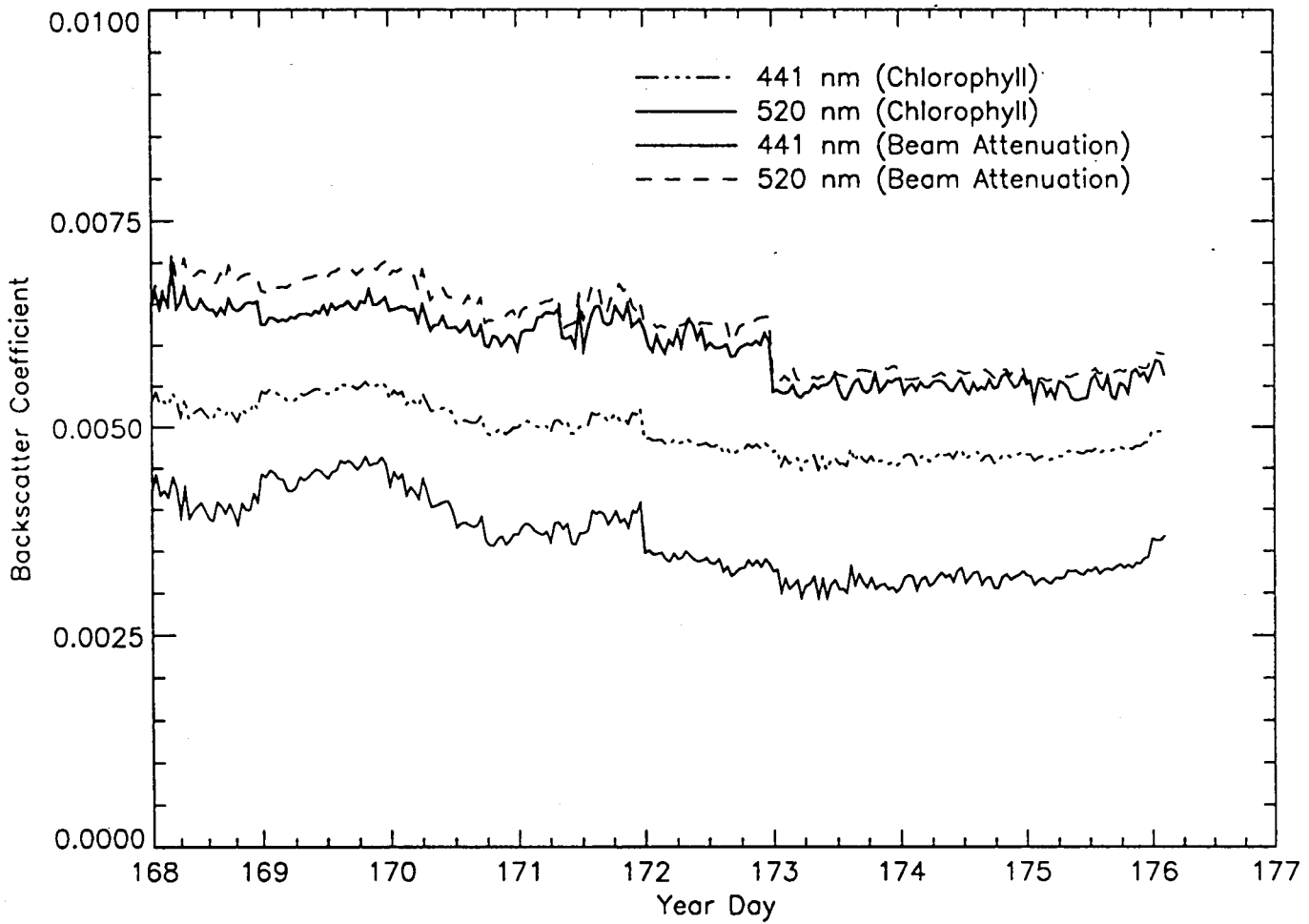
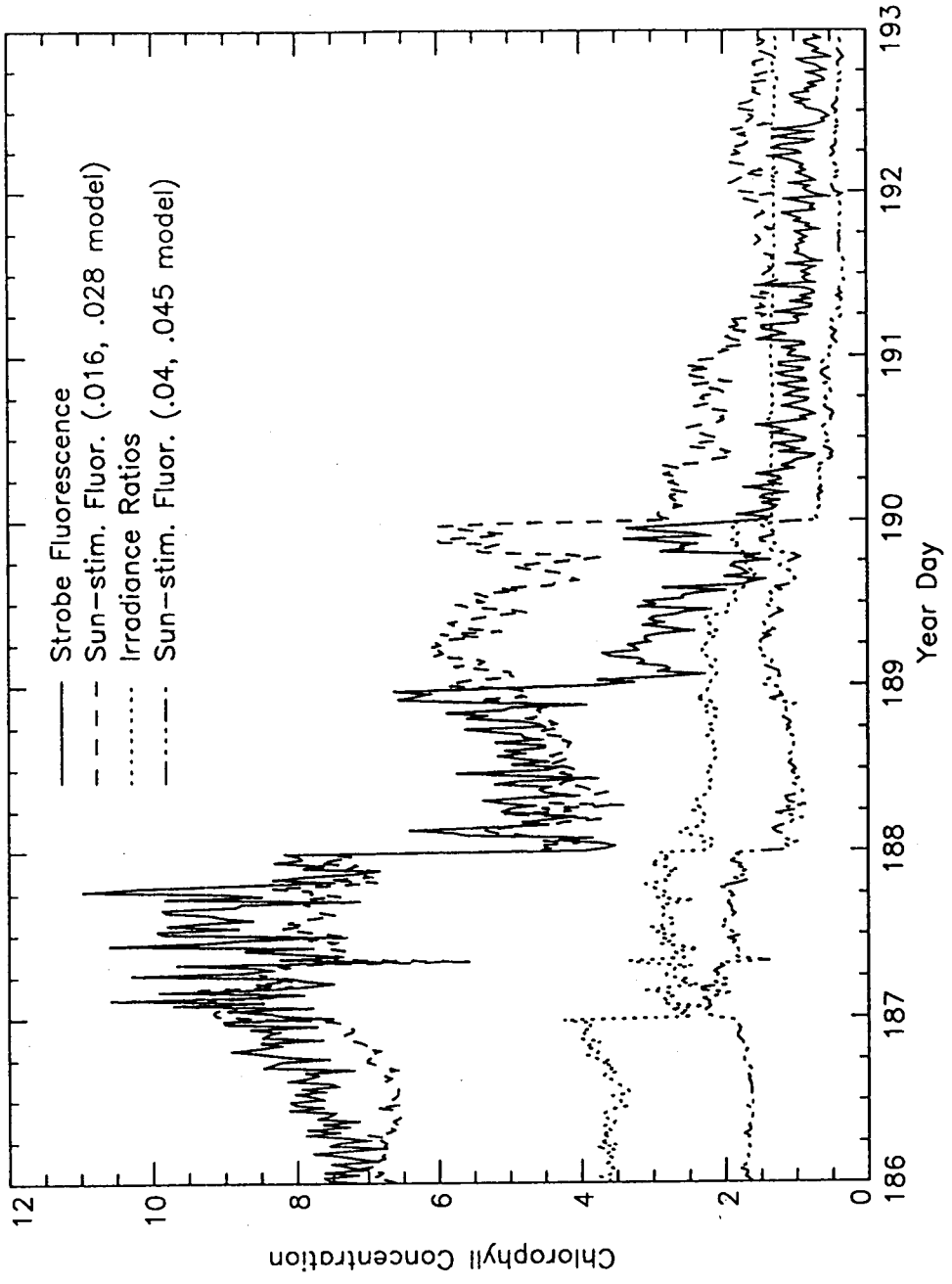


Fig. 5



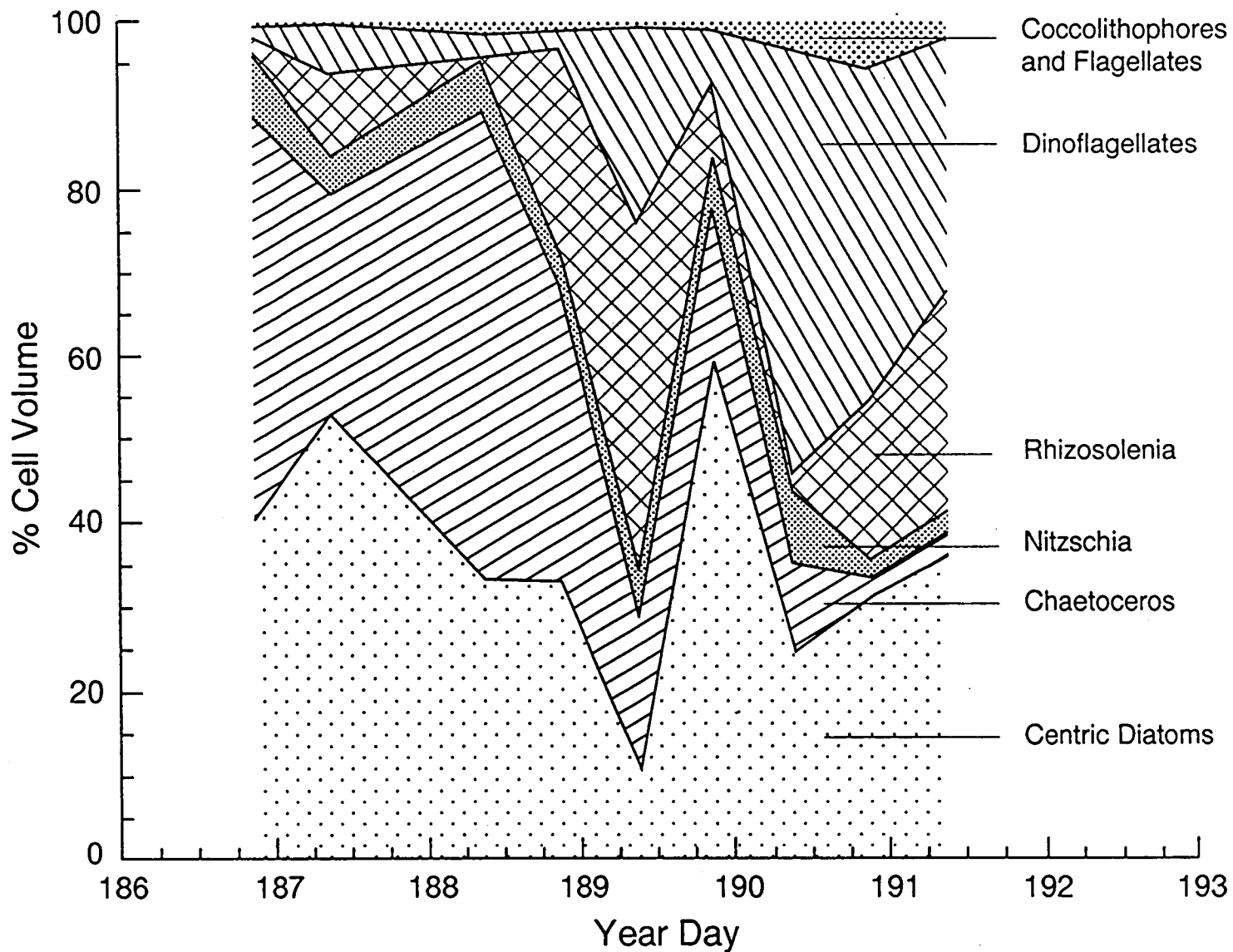
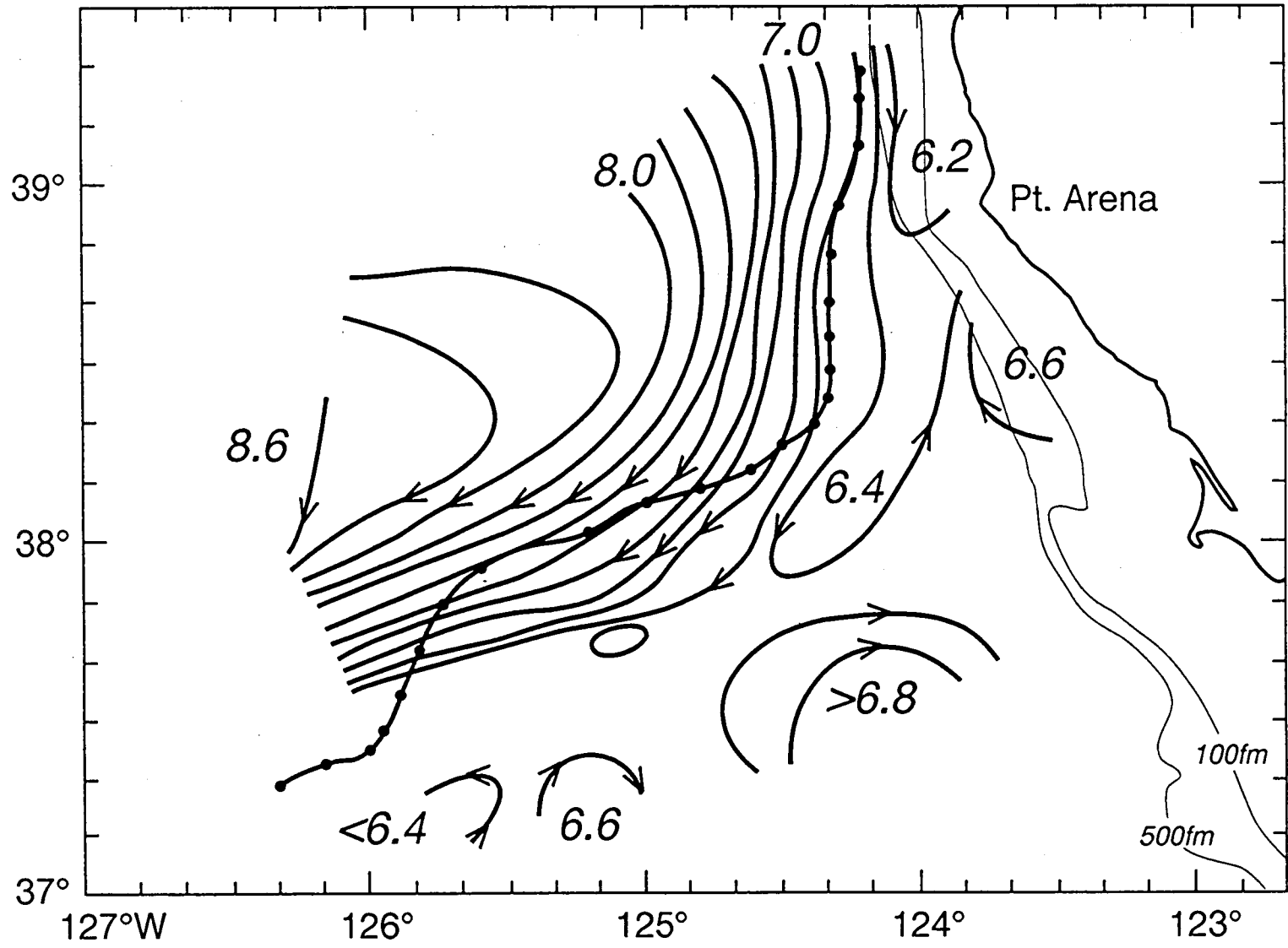
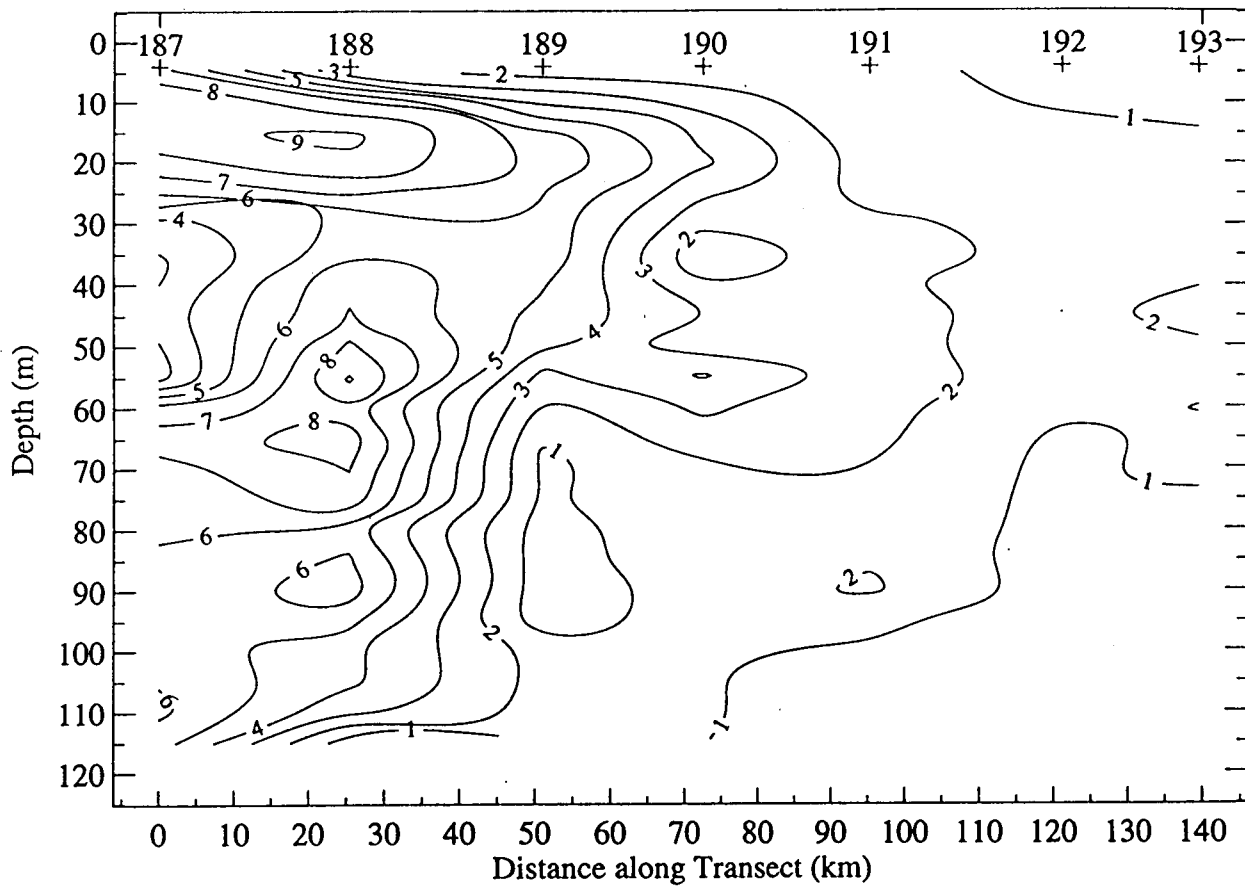
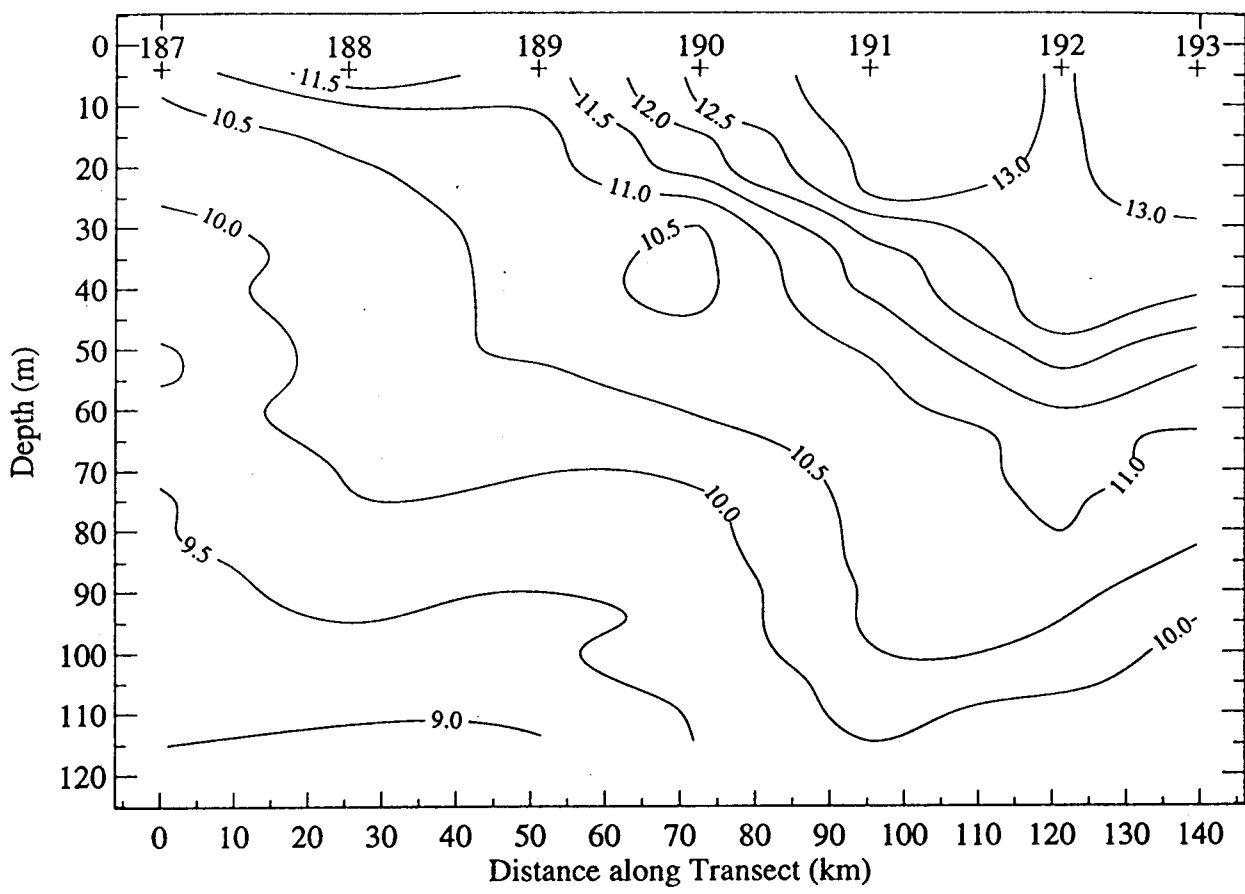


Fig. 7







F.S. 9A

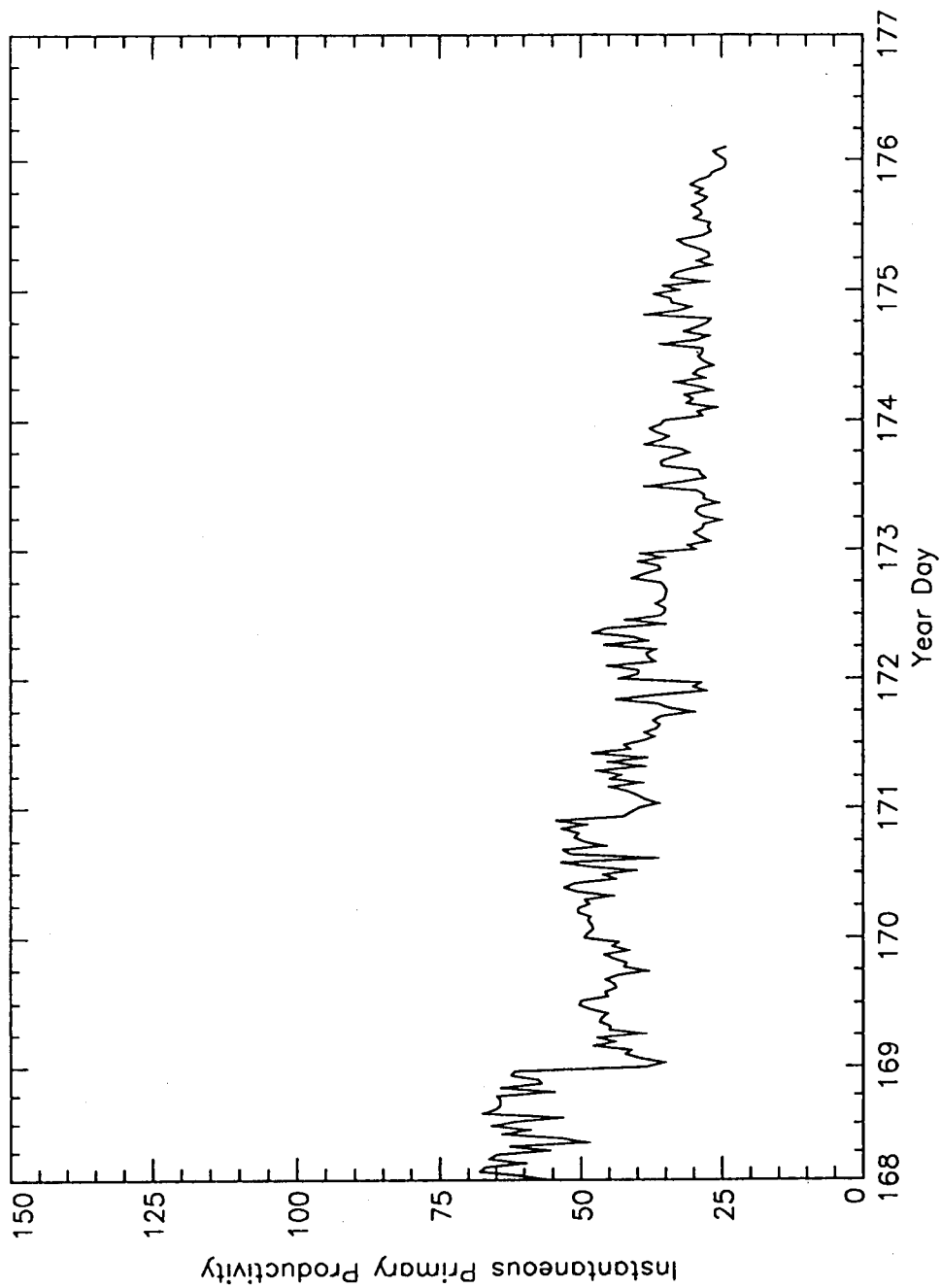


Fig. 9B

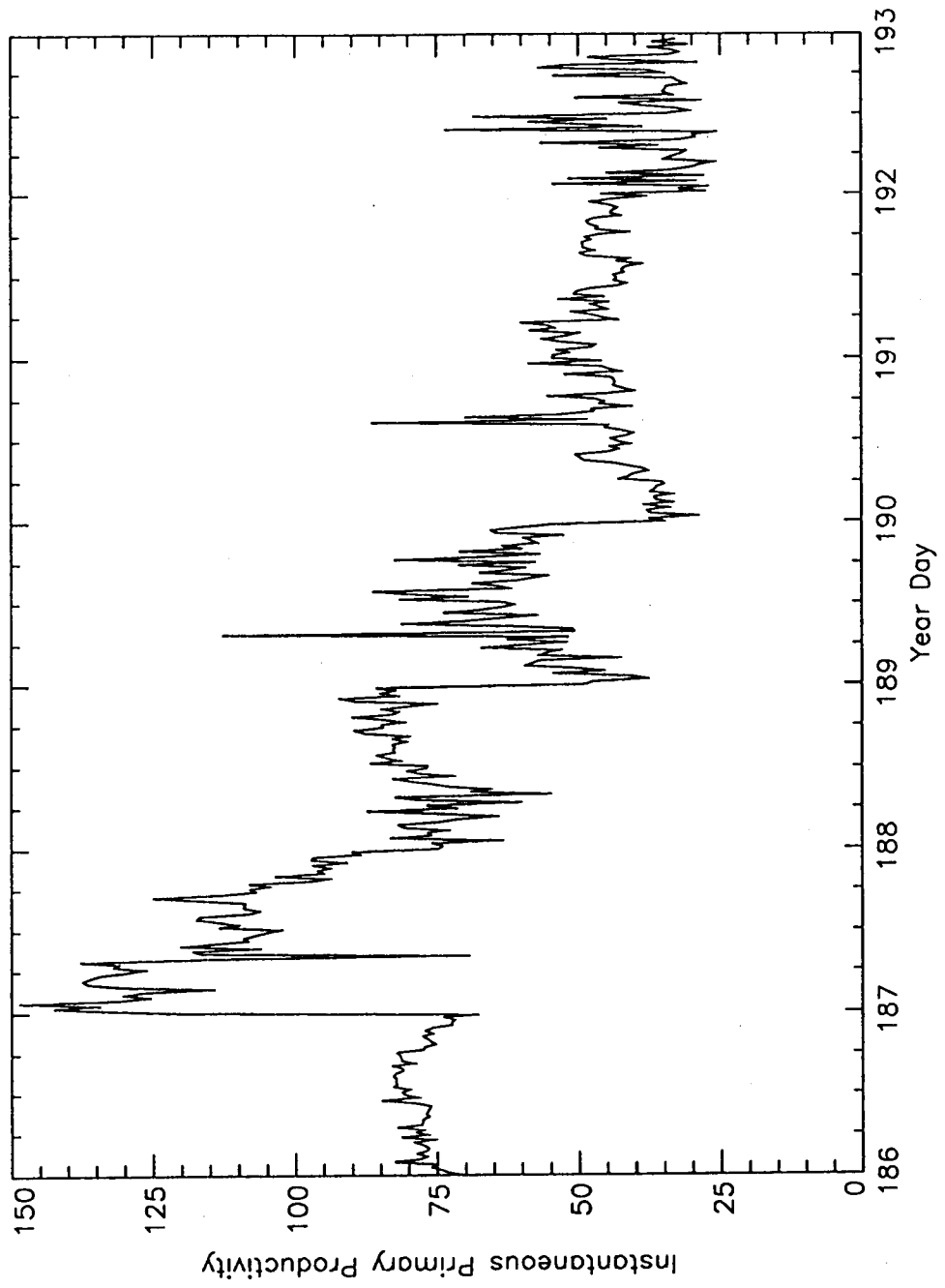


Fig. 10A

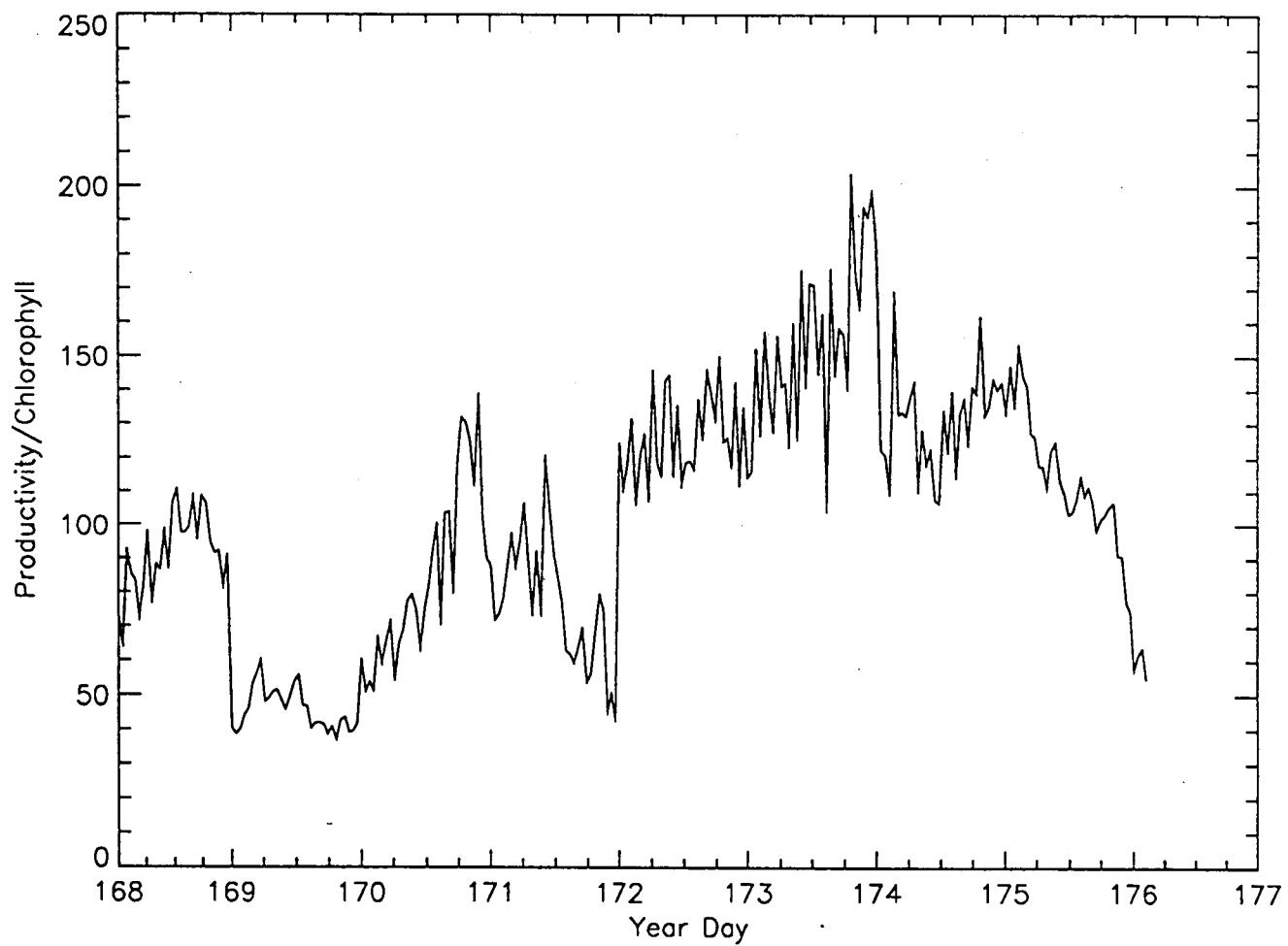


Fig. 10B

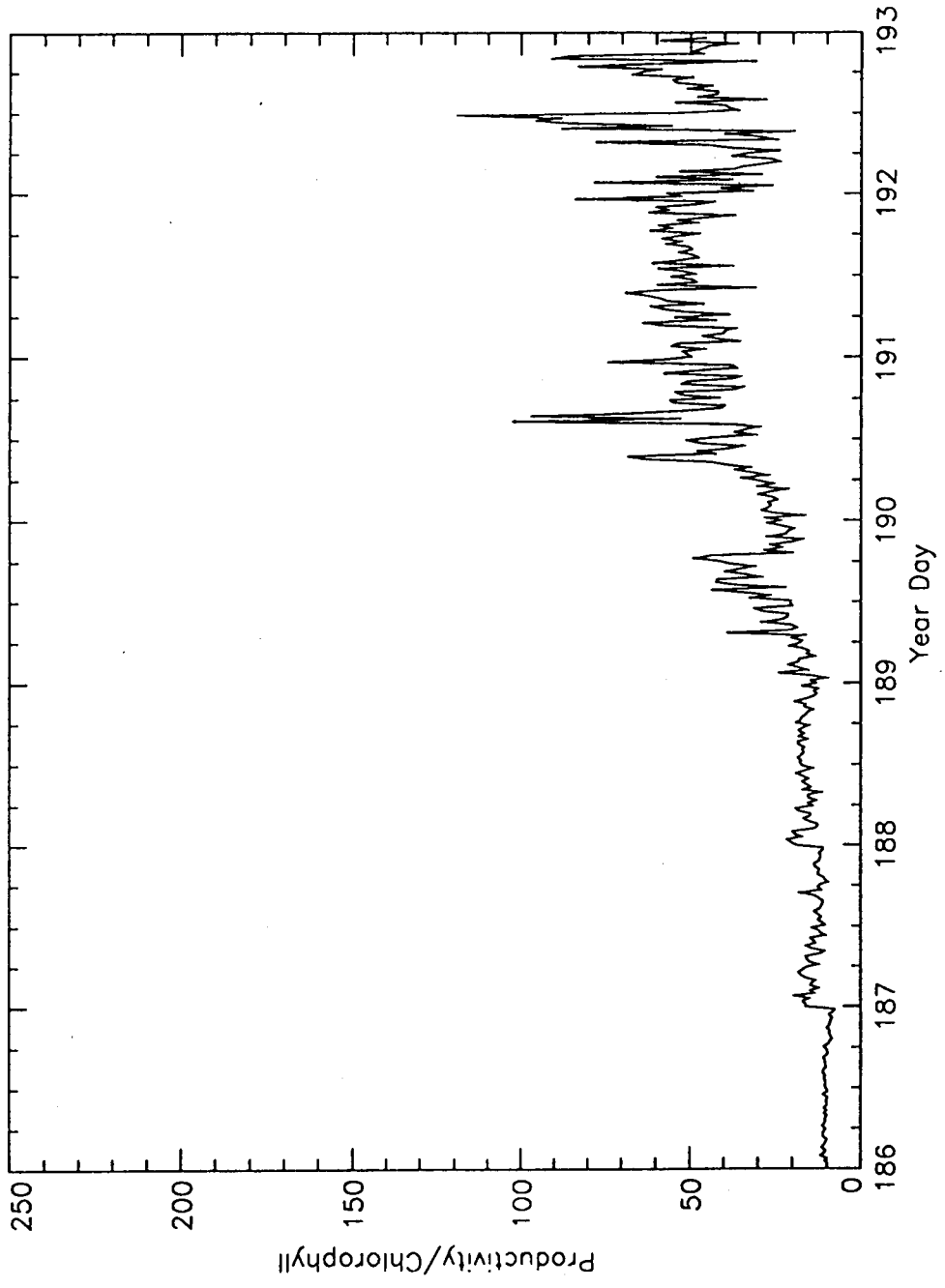
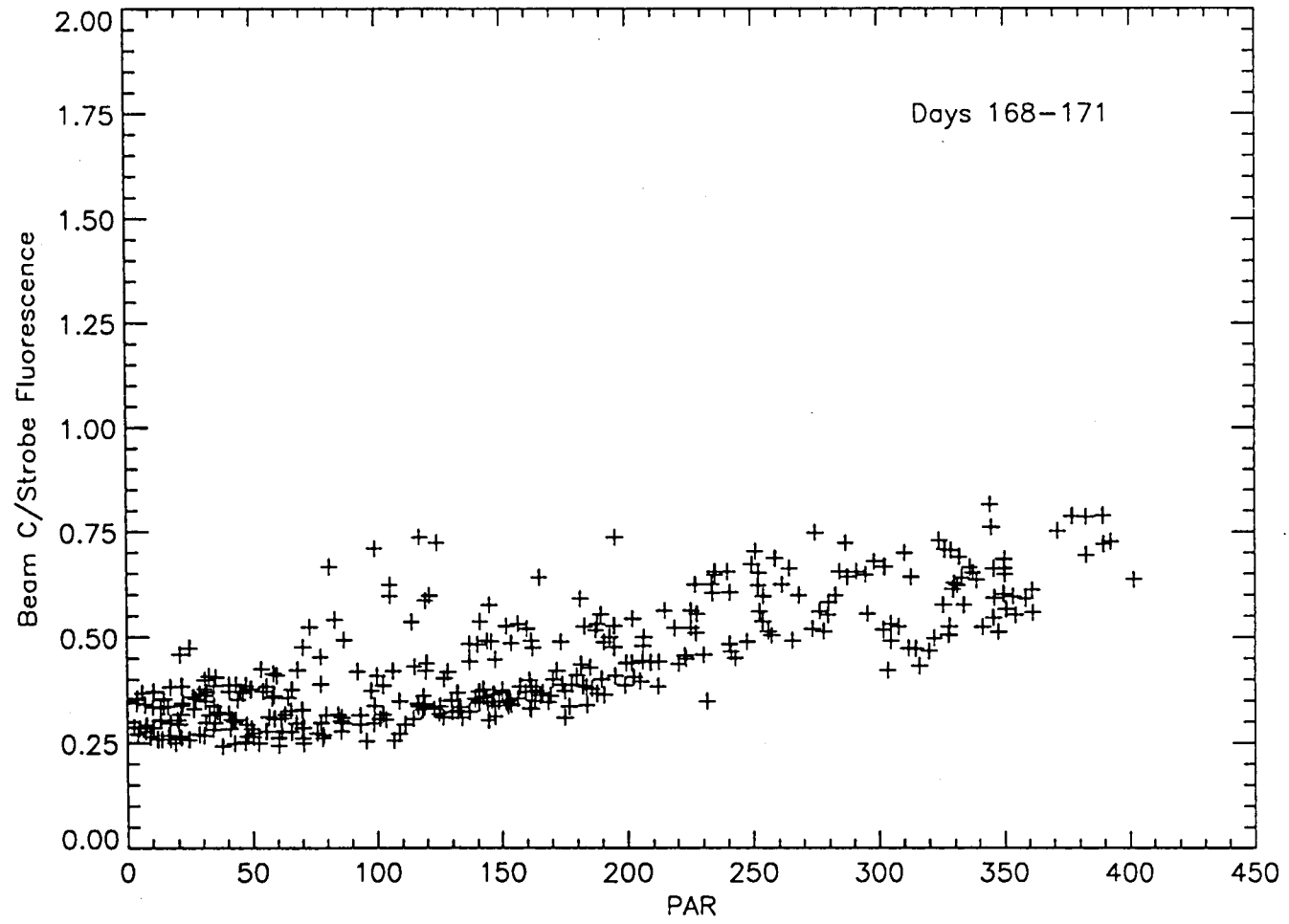


Fig. 11



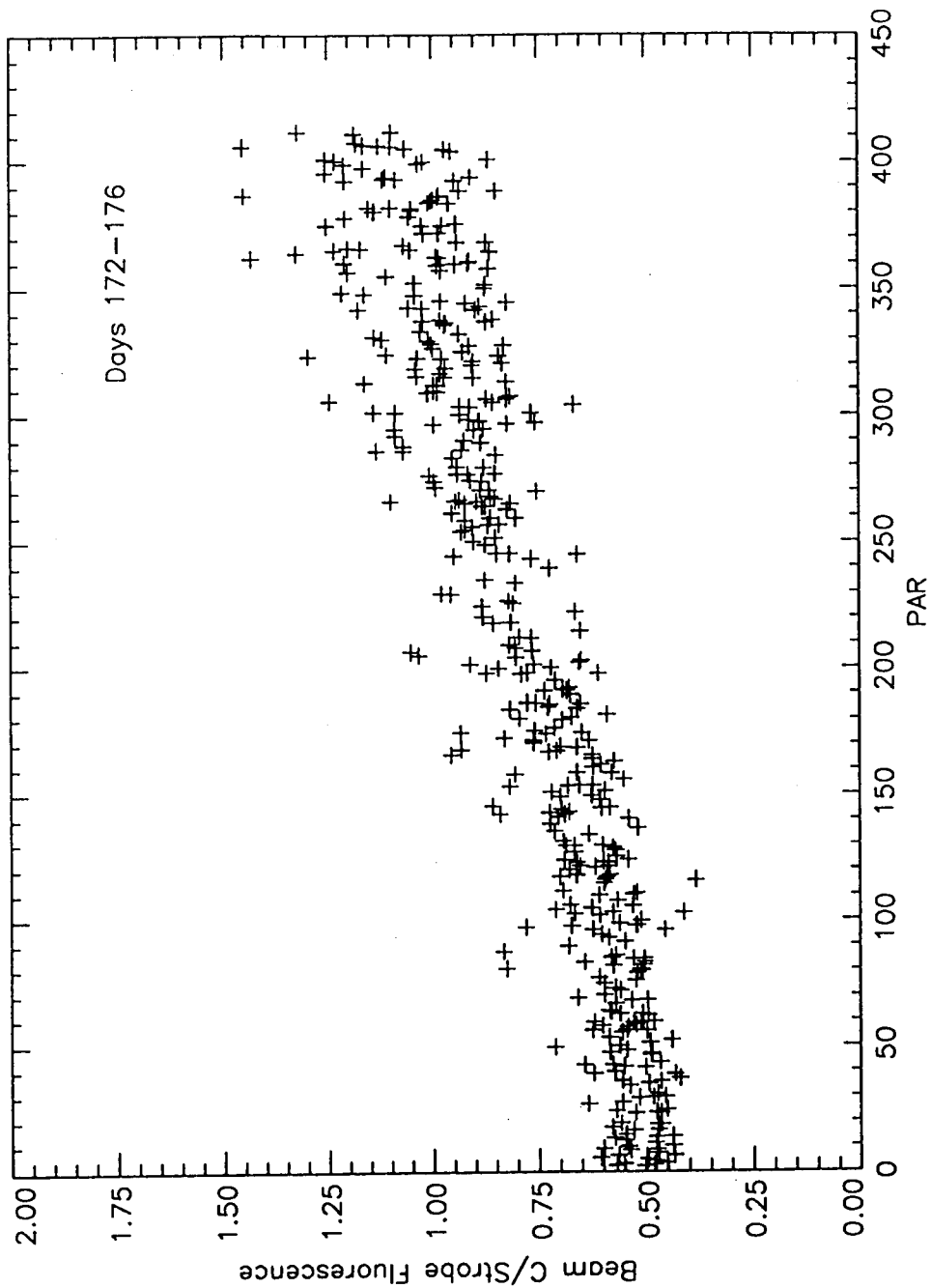


Fig. 12

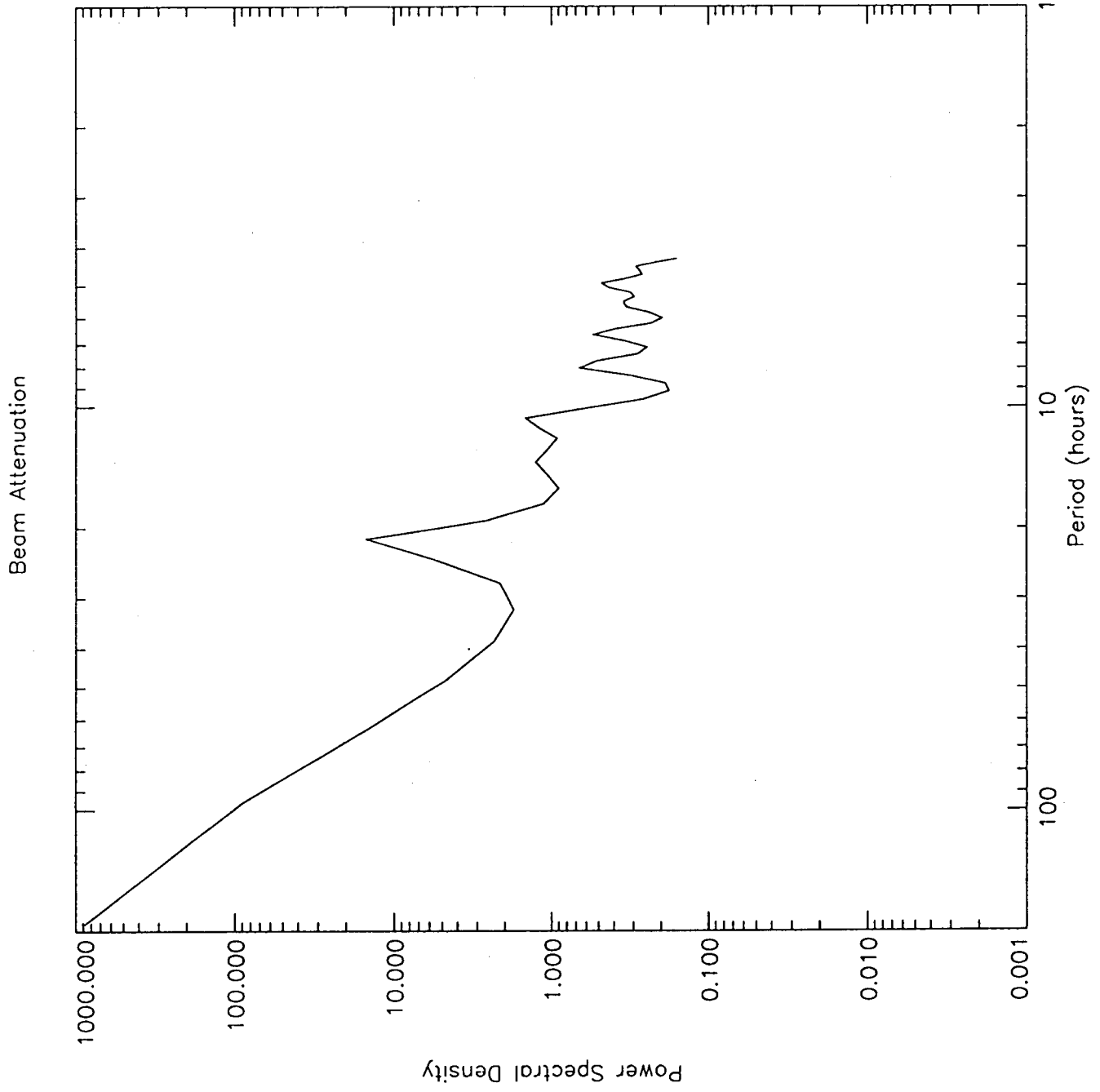


Fig. 13

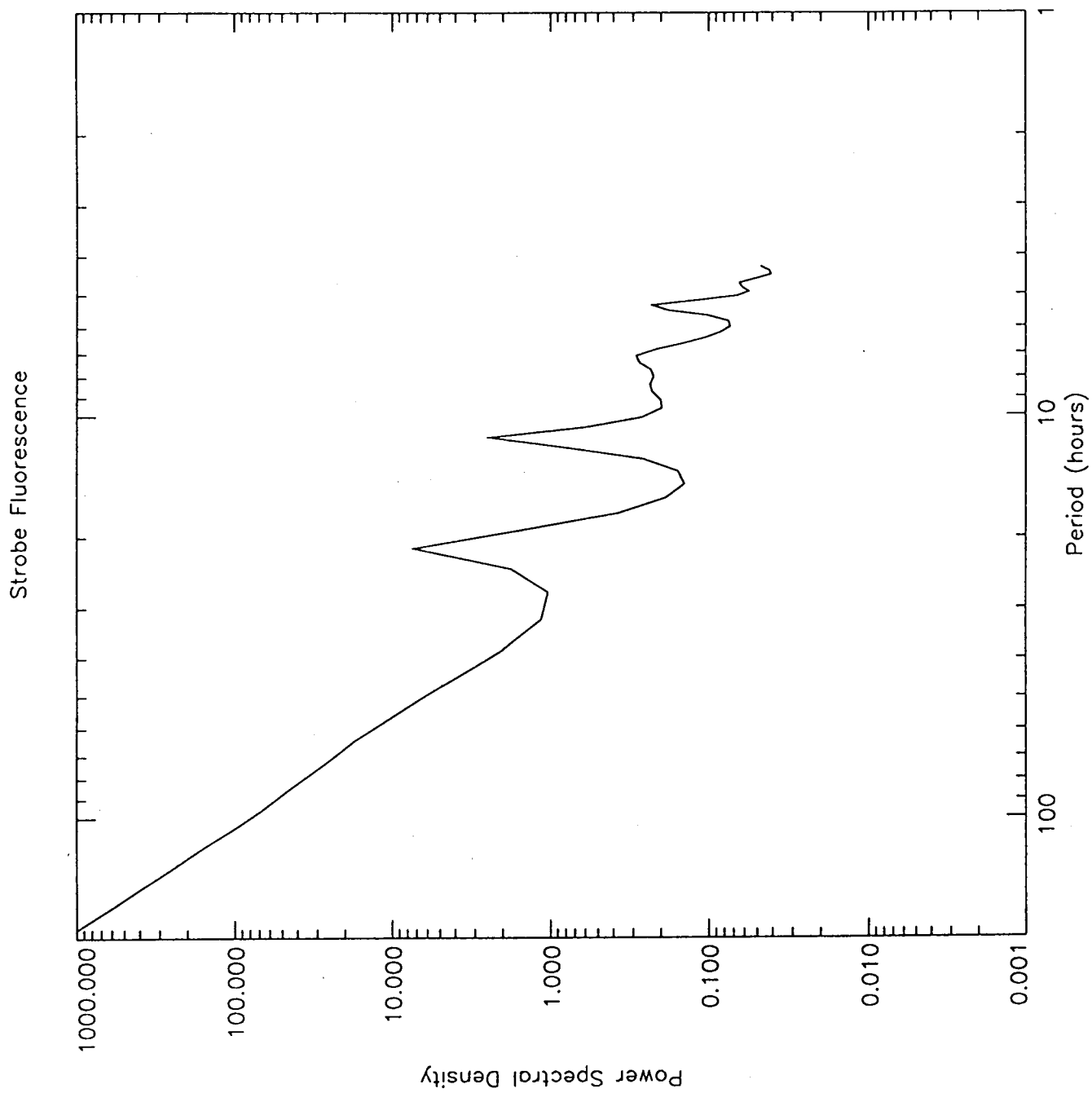


Fig. 14A

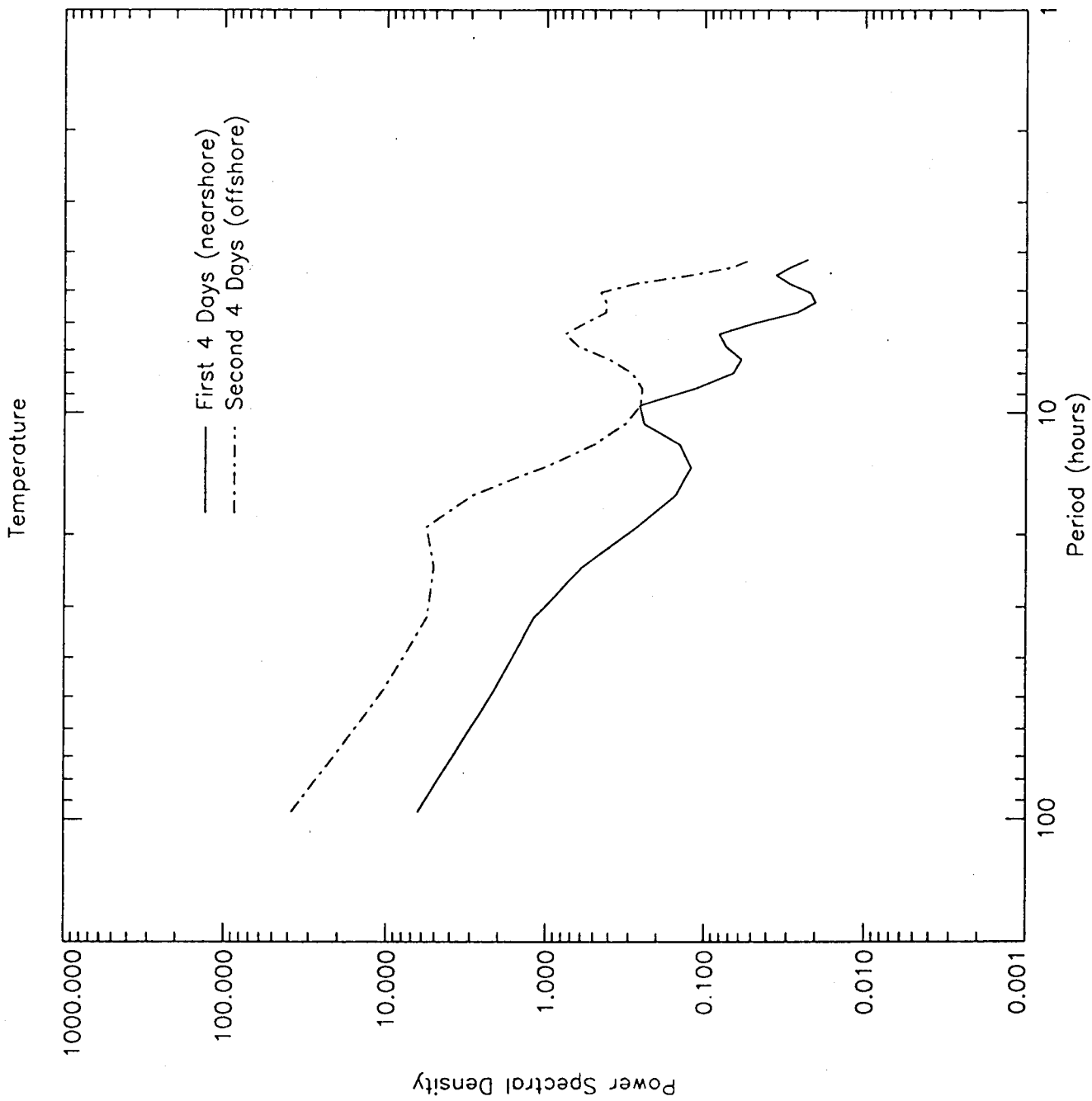
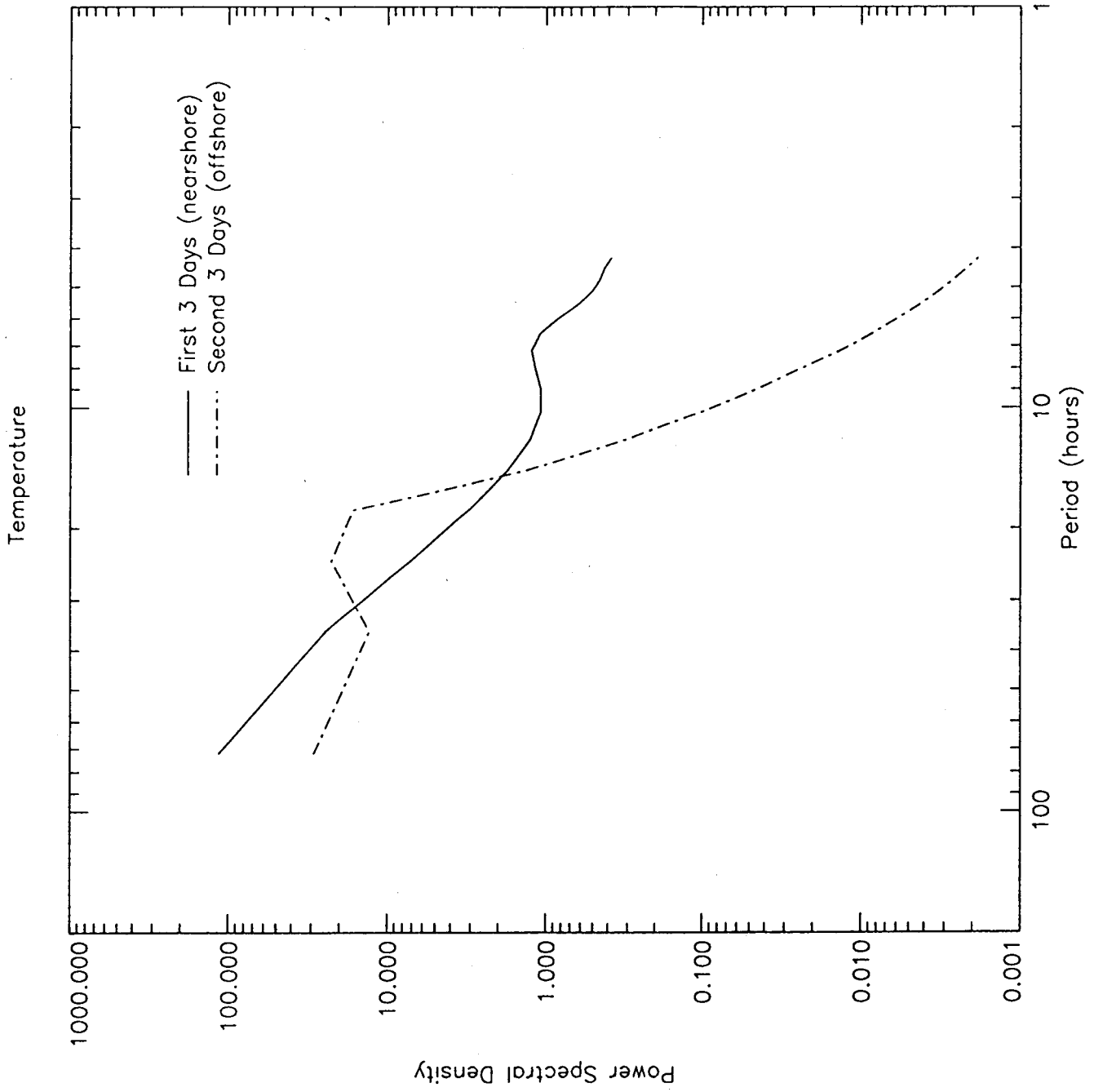


Fig. 14B



5.15

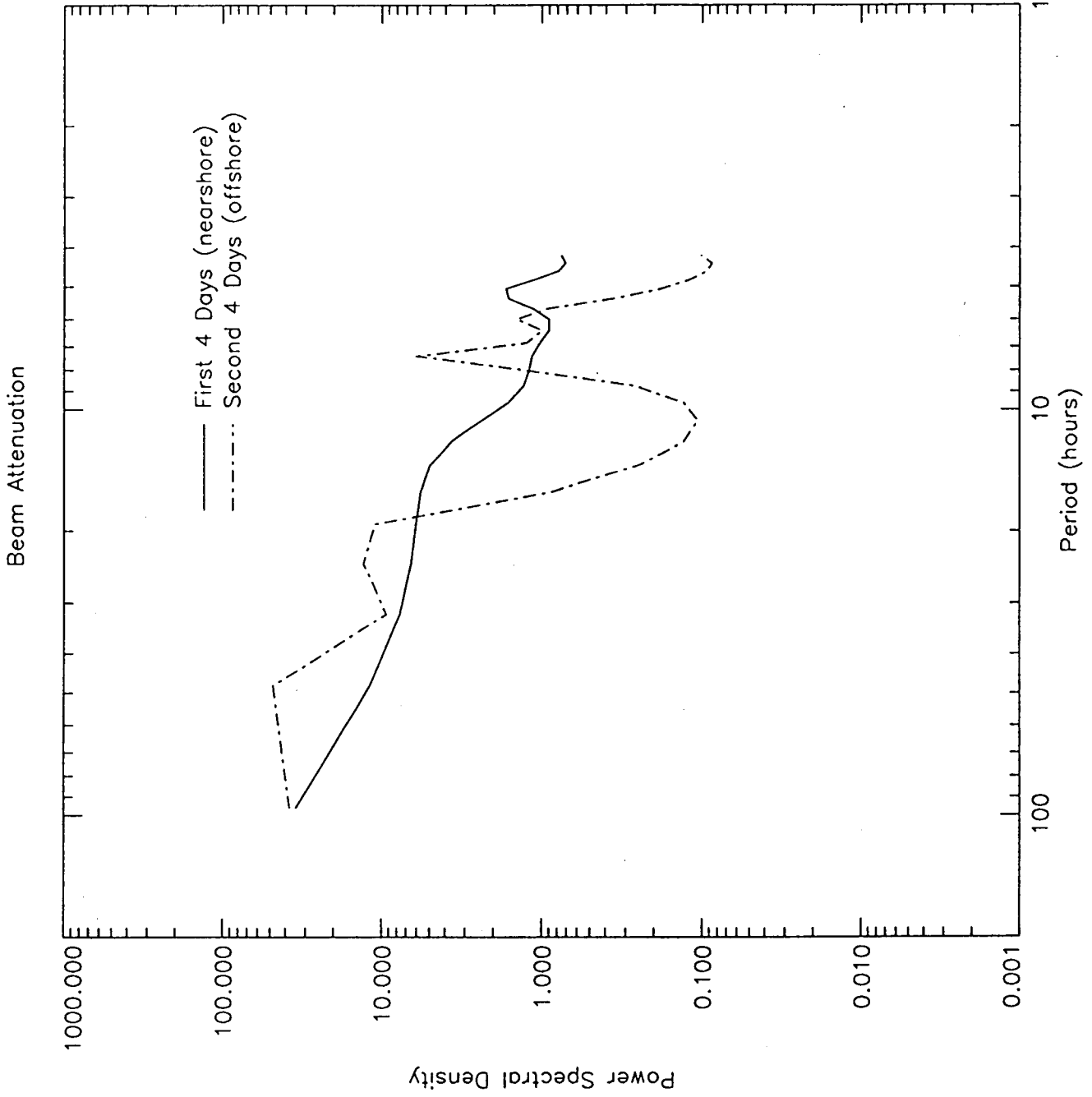


Fig. 16A

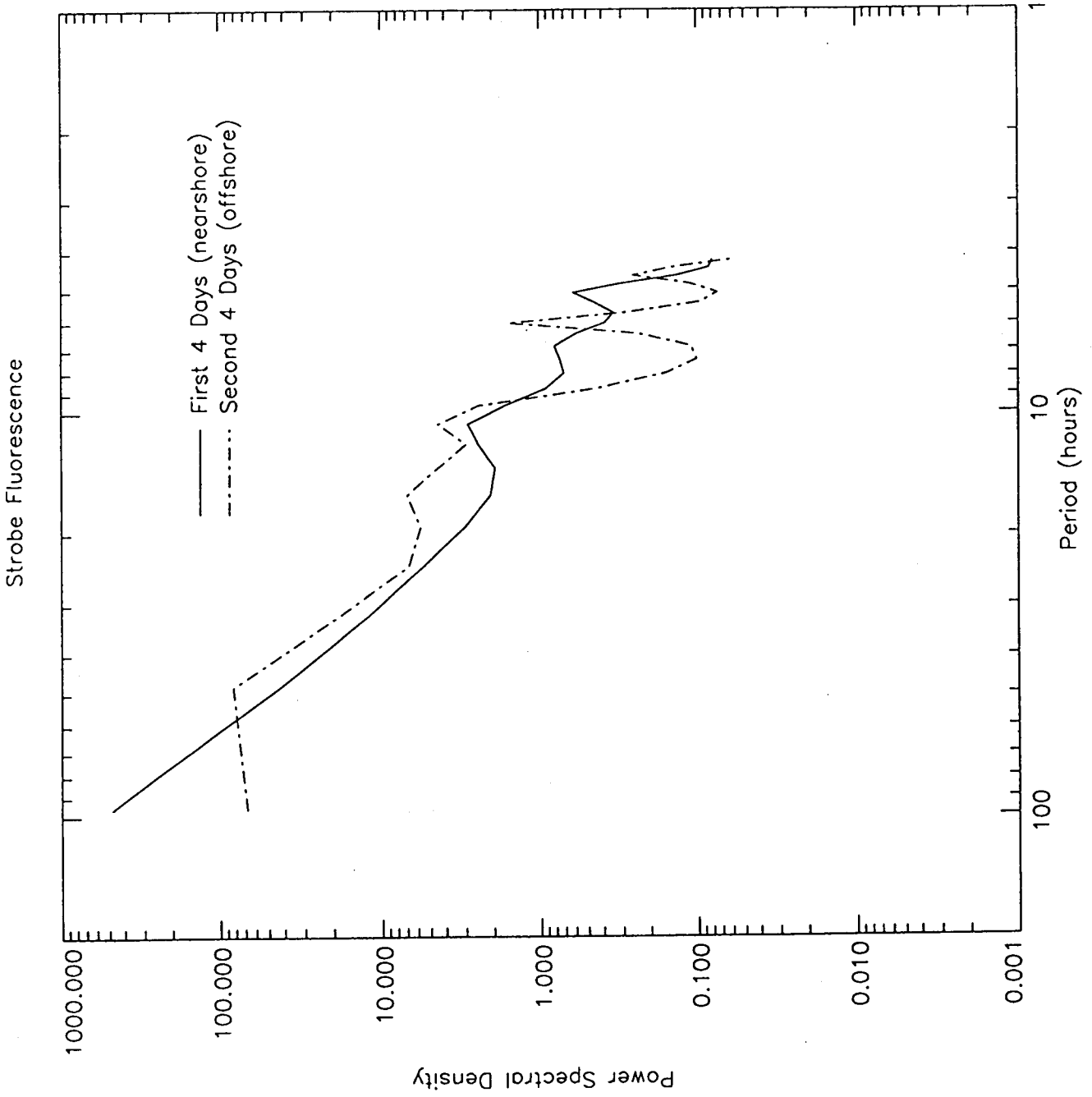


Fig. 16B

